Chem. Senses 24: 351–372, 1999

A Neural Network Model of General Olfactory Coding in the Insect Antennal Lobe

Wayne M. Getz and Antoine Lutz

Division of Insect Biology, ESPM, University of California at Berkeley, CA 94720-3112, USA

Correspondence to be sent to: Wayne M. Getz, Division of Insect Biology, Department ESPM, 201 Wellman Hall, University of California at Berkeley, CA 94720-3112, USA. e-mail: getz@nature.berkeley.edu

Abstract

A central problem in olfaction is understanding how the quality of olfactory stimuli is encoded in the insect antennal lobe (or in the analogously structured vertebrate olfactory bulb) for perceptual processing in the mushroom bodies of the insect protocerebrum (or in the vertebrate olfactory cortex). In the study reported here, a relatively simple neural network model, inspired by our current knowledge of the insect antennal lobes, is used to investigate how each of several features and elements of the network, such as synapse strengths, feedback circuits and the steepness of neural activation functions, influences the formation of an olfactory code in neurons that project from the antennal lobes to the mushroom bodies (or from mitral cells to olfactory cortex). An optimal code in these projection neurons (PNs) should minimize potential errors by the mushroom bodies in misidentifying the quality of an odor across a range of concentrations while maximizing the ability of the mushroom bodies to resolve odors of different quality. Simulation studies demonstrate that the network is able to produce codes independent or virtually independent of concentration over a given range. The extent of this range is moderately dependent on a parameter that characterizes how long it takes for the voltage in an activated neuron to decay back to its resting potential, strongly dependent on the strength of excitatory feedback by the PNs onto antennal lobe intrinsic neurons (INs), and overwhelmingly dependent on the slope of the activation function that transforms the voltage of depolarized neurons into the rate at which spikes are produced. Although the code in the PNs is degraded by large variations in the concentration of odor stimuli, good performance levels are maintained when the complexity of stimuli, as measured by the number of component odorants, is doubled. When excitatory feedback from the PNs to the INs is strong, the activity in the PNs undergoes transitions from initial states to stimulus-specific equilibrium states that are maintained once the stimulus is removed. When this PN–IN feedback is weak the PNs are more likely to relax back to a stimulus-independent equilibrium state, in which case the code is not maintained beyond the application of the stimulus. Thus, for the architecture simulated here, strong feedback from the PNs onto the INs, together with step-like neuronal activation functions, could well be important in producing easily discriminable odor quality codes that are invariant over several orders of magnitude in stimulus concentration.

Introduction

Visual and auditory signals, as well as mechanosensory stimuli, can be precisely characterized by physical measurements of amplitude, direction and, in case of the first two, frequency (electromagnetic or air pressure waves). Chemosensory stimuli, on the other hand, are much more difficult to characterize using a few well-defined measures. A good measure of chemical signal amplitude does exist (i.e. chemical concentration) but, unlike vision (e.g. color) or hearing (e.g. pitch), not of signal quality. Further, chemosensory stimuli cannot easily code spatial information over great distances, primarily because the signals are molecules transported by turbulent air or water plumes that break the signal up into discrete packages with increasing distance from the source (Murlis, 1986; Moore and Atema, 1991; Dittmer *et al.*, 1995). Thus olfactory signals are much noisier than other sensory modalities, which makes the olfactory signal processing problem much different from that, say, of vision (Osorio *et al.*, 1994) or audition.

Olfactory processing is primarily a signal classification problem that is complicated by the fact that olfactory receptor neurons (ORNs) exhibit (i) phaso-tonic response profiles over time; (ii) highly nonlinear stimulus–response relationships with respect to concentration (Akers and Getz, 1992, 1993; Getz and Akers, 1993, 1994; Lemon and Getz, 1997); and (iii) synergistic and inhibitory responses to blends compared with the response to the individual components of blends (Atema *et al.*, 1989; Derby *et al.*, 1989; Fine-Levy and Derby, 1992; Getz and Akers 1995, 1997; Kang and Caprio, 1997). Olfactory processing can also be a spatial information processing problem including transforming temporal information related to the change in the frequency with which an organism is stimulated by discrete

packets of molecules transported in turbulent flows into information on the direction and closeness of an odor source (Moore and Atema, 1988; Murlis *et al.*, 1992).

The noise in odor signals and nonlinearities in the responses of sensory neurons at the periphery challenges our ability to unravel olfactory coding in the animal brain. This challenge, however, cannot be met by prevailing olfactory coding paradigms which have their origins in pheromonal processing in insects (reviewed in Kaissling, 1987; Masson and Mustaparta, 1990). In such pheromonal processing, each compartment of the multicompartment macroglomerular complex (MGC) that is situated in the antennal lobes receives input from only one type of extremely narrowly tuned receptor neuron (Hanson *et al.*, 1992, 1994). The MGC represents an architecture of dedicated pathways, where each pathway is specific for a particular odorant component of the pheromonal blend. This architecture has led to the concept of a 'labeled-line' code in the insect brain—a code which has proved inadequate in describing general olfactory processing in cockroaches (Sass, 1978; Selzer, 1984) and honey bees (Vareschi, 1971; Akers and Getz, 1992, 1993). Unlike pheromonal coding, general odor coding involves peripheral receptor neurons that are tuned to an array of odorants, usually belonging to a related family of compounds (e.g. alcohols, esters, ketones: see Selzer, 1984; Fujimura *et al.*, 1991; Akers and Getz, 1992; Getz and Akers, 1993). The broader response spectrum of general receptor neurons requires that we generalize the notion of dedicated labeled lines: too few labeled lines exist to account for all the possible odorants that insects such as cockroaches and honey bees are able to perceive. The obvious generalization is to consider the code in terms of the across fiber patterns in a cable of neurons relaying information from one part of the insect brain to another (Ache, 1991; Boeckh *et al.*, 1990). Unfortunately, across fiber patterns all too often are thought of in terms of average firing rates in each neuron among a group of neurons thought to produce or transmit an olfactory code.

More recently, Laurent and co-workers (Laurent, 1996; Laurent *et al.*, 1996) proposed the concept of a combinatorial code in terms of the average firing rate over several subintervals comprising the total interval of time over which coding occurs. This paradigm arose because Laurent and colleagues (Laurent and Davidowitz, 1994; Laurent and Narghi, 1994; Laurent, 1996; Laurent *et al.*, 1996; MacLeod and Laurent, 1996; Wehr and Laurent, 1996) found activity in projection neurons from the antennal lobe of insects correlated with 20 Hz local field potential oscillations in the insect mushroom bodies where sensory modalities are mixed and long-term memory is known to occur (Menzel *et al.*, 1991). This type of combinatorial paradigm, however, is essentially an extension of the across fiber pattern paradigm: instead of having n numbers (or states) associated with a code across n neurons, one has $n \times m$ numbers if the coding interval of time is divided into m subintervals.

A deeper understanding of the code can only be obtained if we move away from static or combinatorial paradigms to temporally varying (i.e. dynamical systems) paradigms. Temporally varying concepts of coding take cognizance of the dependence of the phasic activity of the coding neurons on initial conditions that, with time, become less important as the stimulus-specific neuronal states are approached. A combinatorial paradigm raises the critical question of how long an odor coding interval is (e.g. if the coding interval were 500 ms, then in the context of 20 Hz oscillations this would imply $m = 10$). Also, does the early part of the response of the coding neurons (i.e. the first or first few subintervals) reflect initial brain states rather than stimulus-specific brain states?

The only way to explore the properties of a temporally varying coding paradigm is through the analysis of appropriate dynamic neural network models. Here, we carry out such an analysis using a model that reflects the underlying architecture of the olfactory components of the insect antennal lobe. The function of each of these olfactory components, however, cannot be teased apart unless we start with a reasonably simple model and explore changes in the behavior of the model as complexity is added. Once this is accomplished, the model can be made more realistic using known anatomical and physiological features of the insect olfactory system.

More attention has been devoted to modeling vertebrate or generic olfactory systems than insect olfactory systems (e.g. see Freeman and Skarda, 1985; Baird, 1986; Getz and Chapman, 1987; Skarda and Freeman, 1987; Barnard, 1989; Li and Hopfield, 1989; Granger *et al.*, 1990; Bower, 1991; Getz, 1991, 1994; Hopfield, 1991; Wang *et al.*, 1991; Bhalla and Bower, 1992; Meredith, 1992; Schild and Reidel, 1992; White *et al.*, 1992; Hendin *et al.*, 1994; Aradi and Erdi, 1996; Linster and Hasselmo, 1997). Previous analyses of mammalian (Freeman and Skarda, 1985; Baird, 1986; Skarda and Freeman, 1987; Barnard, 1989; Bower, 1991), amphibian (White *et al.*, 1992), and non-insect invertebrate systems, such as the mollusc, *Limax maximus* (Delaney *et al.*, 1994; Kleinfield *et al.*, 1994), are very different from the analysis presented here because they focus on relatively low frequency oscillations that are observed across sheets of olfactory cortex or analogous invertebrate neuropil (see also Laurent and Davidowitz, 1994; Laurent and Narghi, 1994; Laurent, 1996; Laurent *et al.*, 1996; MacLeod and Laurent, 1996; Wehr and Laurent, 1996).

Olfactory processing in insects has been more widely studied in the context of pheromone detection than general odor detection. General odor detection studies are gaining ground (Fujimura *et al.*, 1991; Akers and Getz, 1992, 1993; Getz and Akers, 1993, 1994, 1995, 1997; Laurent and Davidowitz, 1994; Laurent and Narghi, 1994; Rospars and Fort, 1994; Laurent, 1996; Laurent *et al.*, 1996; MacLeod and Laurent, 1996; Wehr and Laurent, 1996; Joerges *et al.*, 1997; Lemon and Getz, 1997, 1999). The insect antennal

lobe, the part of the insect brain receiving input from olfactory receptor afferents, has a number of underlying architectural features in common with the vertebrate olfactory bulb (Boeckh *et al.*, 1990). Thus, some understanding of the function of the architectural features of the insect antennal lobe should provide insight into olfactory processing in all animals.

The architecture of our model is based on physiological and anatomical data that have been obtained primarily from the American cockroach, worker honey bees, several species of moths (e.g. Rospars, 1983, 1988; Boeckh and Ernst, 1987; Christensen and Hildebrand, 1987; Flanagan and Mercer, 1989a,b; Gascuel and Masson, 1991; Malun, 1991a,b; Hansson *et al.*, 1994) and a few other insects (as reviewed in Smith and Getz, 1994). To date, modeling studies of the insect antennal lobe have focused on reproducing the behavior of specific antennal lobe neurons (Linster *et al.*, 1993, 1994; Linster and Masson, 1996), behavior (Masson and Linster, 1996; Linster and Smith, 1997) or self-organization properties based on a Hopfield recurrent net architecture (Malaka *et al.*, 1996). In some of these models, important architectural details pertaining to the insect antennal lobe have not been considered, although others are more detailed (e.g. Linster and Smith, 1997).

The olfactory information processing questions we address here relate to the role played by the architectural features and response properties of the intrinsic neurons (INs) and projection neurons (PNs) of the insect antennal lobe in solving the 'general olfactory coding problem in insects' defined as follows (cf. Osorio *et al.*, 1994):

> In response to odor stimuli with naturally occurring levels of spatial and temporal variation, the general olfactory coding problem in insects is for the peripheral and antennal lobe neurons to produce responses in a subset of the antennal lobe projection neurons that, as an assembly, exhibit patterns of firing sufficiently similar across a range of concentrations of stimuli of the same quality and sufficiently different among stimuli of different quality to permit an appropriate classifier (either a higher level network such as the mushroom bodies of the protocerebrum or a measure in a linear space, as employed in this proposal) to identify odors of the same quality or to discriminate odors of different quality.

Several issues immediately arise from this definition relating to the temporal properties of the code. The already mentioned relationship between period of oscillations in field potentials (Laurent, 1996; Laurent *et al.*, 1996; MacLeod and Laurent, 1996) and the overall coding interval is one issue. Another is the influence the phaso-tonic response properties of receptor neurons (Akers and Getz, 1992; Lemon and Getz, 1997) may have on the temporal character of odor codes. A third issue is the role that nonlinear response characteristics of receptor neurons [especially inhibitory responses to mixtures compared with pure odorants—see Getz and Akers (1995)] may play in producing olfactory codes. Beyond these are the broader issues of how olfactory systems are able to separate distinct odor signals as they mingle together in the environment or identify the quality of a particular odor from a background of odors. These latter issues have been considered in several modeling studies by Hopfield and collaborators (Li and Hopfield, 1989; Li, 1990; Hopfield, 1991; Hendin *et al.*, 1994) and also in an earlier study by one of us (Getz, 1991). All of these studies, however, employ recurrent autoassociative networks that do not take cognizance of the glomerular neuropil structures characteristic of the insect antennal lobe or vertebrate olfactory bulb.

The issues mentioned above raise questions that probe deeply into the temporal properties of olfactory coding and we are not yet in a position to address all of them. In this study, we shed some light on some of the basic questions raised for systems with constant input stimuli and idealized peripheral ORNs. Studies involving inputs that have temporal, as well as spatial, components can follow once we have obtained some understanding of the computational properties of olfactory systems receiving spatially homogeneous on–off input of the type considered here. We can only account for spatial heterogeniety if we model the input to each glomerulus as coming from several different ORNs each located at a different site (sensillum) on the antennae (cf. Malaka *et al.*, 1996). In this case, the activation of each ORN depends on the structure of the odor plume with respect to the location of the ORNs on the antennae. Our assumption of spatial homogeneity is functionally equivalent to assuming a single input into each glomerulus with a firing rate that increases with concentration.

Network approach

The model we present here to investigate olfactory processing in the insect brain can be viewed as a generalization of the subsystem architecture studied by Av-Ron and colleagues (Av-Ron and Rospars, 1995; Av-Ron and Vibert, 1996). They consider several special cases of two ORNs synapsing with two local INs which in turn synapse with one or two PNs, and they model the activity of these neurons using four differential equations to describe the currents producing the associated activation potentials (Av-Ron *et al.*, 1991; Wang and Rinzel, 1992). Av-Ron and colleagues, however, do not include any feedback from the PNs onto the INs. As we will see, our results suggest that this PN–IN feedback may be an important component of the olfactory coding processes in the insect antennal lobe.

In developing our model, we follow the dictum that 'a good model should not copy reality, it should help to explain it' (Segev, 1992). In particular, we seek insights into the type of code produced by a set of input ORNs synapsing on an underlying net of INs from which a set of

uniglomerular PNs project. To keep the model simple, however, we only use one differential equation to characterize the activation potential in each neuron, so that the output from our net is in terms of the probability that each of the PNs is spiking at a particular point in time, rather than the details of the actual spike trains themselves. This approach leads to formulating a set of n ordinary differential equations for a network containing n neurons (Appendix A). The equations include parameters that characterize the value of the response threshold, the steepness of the neuronal activation function and the background firing rate for each neuron, as well as the value of the connectance parameters (synapse strengths both positive for excitatory connections and negative for inhibitory connections) among neurons.

Antennal lobe architecture

The olfactory neuropil in the antennal lobe of the insect deutocerebrum can be thought of as an olfactory processing 'black box' that receives input from peripheral ORNs located in the antenna and produces output in relay neurons (i.e. PNs) that project from the antennal lobe to higher processing centers in the protocerebrum (reviewed by Rospars, 1988; Masson and Mustaparta, 1990; Hildebrand and Shepherd, 1997) (Figure 1).

Considerable progress has been made in characterizing the anatomy and physiology of the insect antennal lobe (Arnold *et al.*, 1985; Boeckh and Ernst, 1987; Christensen and Hildebrand, 1987; Malun, 1991a,b; Rospars, 1988; Flanagan and Mercer, 1989b; Gascuel and Masson, 1991; Christensen *et al.*, 1993; Hansson *et al.*, 1994), although certain critical neurological questions remain unanswered (e.g. whether certain neurons intrinsic to the antennal lobe are uni- or bi-directional). Also, the general function of the antennal lobe is not well understood, although some progress has been made in terms of the MGC in the antennal lobes of certain species of moth (Hansson *et al.*, 1992, 1994). The inputs to the antennal lobes are olfactory ORN axons that arborize in the antennal lobe glomeruli, which are grape-like neuropil structures enclosed by a sheath of glial cell process (Homberg *et al.*, 1989; Boeckh *et al.*, 1990; Masson and Mustaparta, 1990; Gascuel and Masson, 1991; Christensen *et al.*, 1993). These arborizations synapse almost exclusively with INs that interconnect several glomeruli, but remain intrinsic to the antennal lobe. All INs identified thus far appear to be inhibitory [they are GABA-ergic—but see Michelson and Wong (1991), for examples of excitatory GABA-ergic neurons]. The INs synapse with the dendrites of the PNs which, in turn, appear to synapse back onto the INs before they exit a glomerulus (Malun, 1991a,b), thereby forming possible excitatory–inhibitory feedback loops that parallel granule–mitral cell feedback loops in the vertebrate olfactory bulb (e.g. Li and Hopfield, 1989; Shepherd, 1994, Figure 7.17; Yokoi *et al.*, 1995; Erdi *et al.*, 1997).

Besides providing the backbone to the glomerular network, the network of INs informationally link all the glomeruli, although each individual IN may only synapse with neurons in a small proportion of the total number of glomeruli. Even in species that have large MGCs, such as the male sphinx and turnip moths, INs exist that arborize throughout the entire antennal lobe, including the MGC (Christensen *et al.*, 1993; Hansson *et al.*, 1994). At this time, it is not known if some or all INs have input regions in one glomerulus and output regions in several others, or as mentioned are bi-directional in terms of current flow. Some of these INs appear to be symmetric in the sense of arborizing with the same intensity in all the glomeruli they invade, while others have the asymmetry of arborizing intensely in only one of the glomeruli and less intensely in others (Flanagan and Mercer, 1989a; Fonta *et al.*, 1991, 1993; Christensen *et al.*, 1993). This apparent asymmetry, however, could be an artifact of incomplete filling of neurons with dyes when using a pipette technique.

In the honey bee and cockroaches, the ordinary glomeruli give rise to one uniglomerular PN, but are also invaded by multiglomerular PNs. In all insects, however, the MGC gives rise to several uniglomerular PNs. In the cockroach, only the male has an MGC (Boeckh *et al.*, 1990), which gives rise to ~15 PNs (Boeckh and Ernst, 1987). In the honey bee, drones have an MGC consisting of four large glomeruli, queens have one enlarged glomerulus and workers have only ordinary glomeruli [~166 of them—see review by Masson and Mustaparta (1990)]. MGCs are implicated in pheromonal processing (reviewed by Rospars, 1988; Masson and Mustaparta, 1990; Hildebrand and Shepherd, 1997), while the regular glomeruli are associated with general odor processing. Thus the firing patterns across the uniglomerular PNs from the ordinary glomeruli provides a convenient representation of the output of the antennal computation involving floral and food odor stimuli (Getz and Chapman, 1989; Smith and Getz, 1994). Odor responsive multiglomerular PNs also exist (Fonta *et al.*, 1993), but they appear to invade only the 'core', not the 'periphery', of the glomeruli where they can feed information back to the INs (Malun, 1991a,b). Thus, to begin, it makes sense to concentrate on the set of uniglomerular PNs as representing one level of ouput from the olfactory lobe. The additional complexity of multiglomerular PNs can be considered once a deeper understanding of the uniglomerular subsystem has been obtained.

Architecture of the model

The basic architectural features of the insect olfactory system outlined above are schematized in Figure 1. In this study, to keep the model simple, we consider only one class of INs, although more than one class appears to exist (e.g. see Sun *et al.*, 1993), as mentioned above. In particular, we assume that the jth IN receives excitatory input from all the antennal (peripheral) ORNs that project into the jth glomerulus and also receives feedback from the jth PN (the

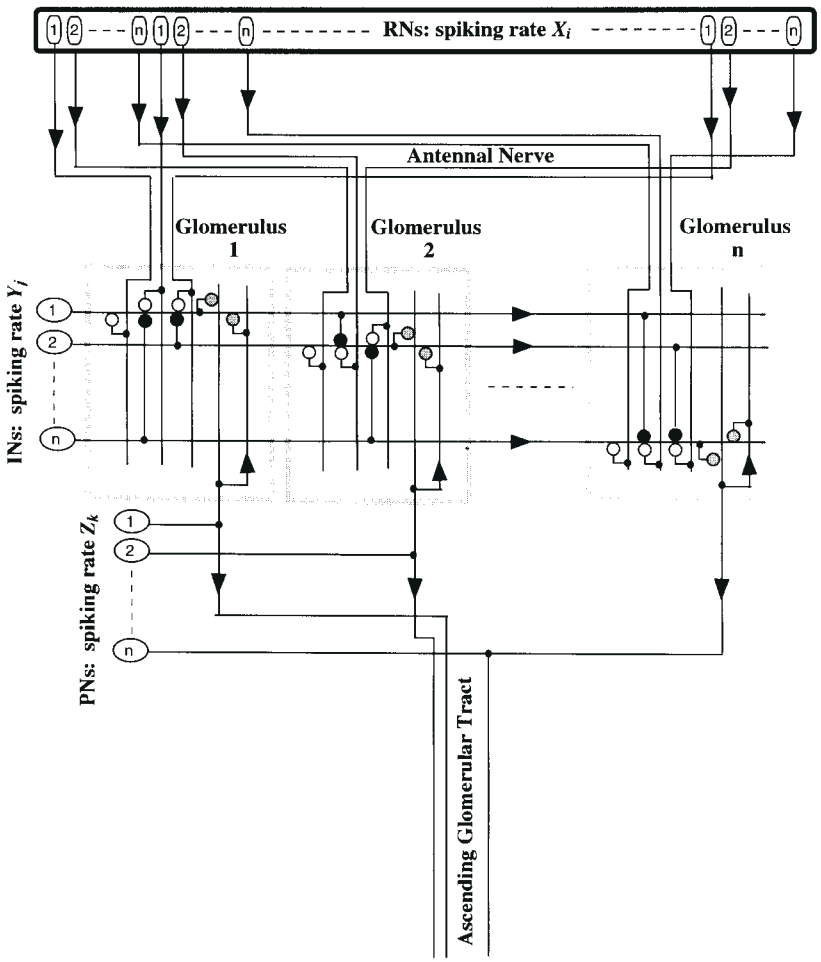

Figure 1 A schematic of the architecture underlying the neural system modeled by equations (4) (Appendix A). The circles represent the four types of synapses: receptor neuron (RN) excitatory feedforward onto interneurons (INs) (w_{ij}, open circles); IN inhibitory feedforward onto other INs (w_{qj}, solid circles: if $w_{jj} \neq 0$ then we have IN feedback onto itself, which is not considered here); IN inhibitory feedforward onto projection neurons (PNs) ($\overline{w}_k$, stippled circles); and PN excitatory feedback onto Ins (w_j, cross-hatched circles). Note, as discussed in the text, each PN fires through disinhibition of a self or implicit excitation process (Christensen *et al.*, 1993).

PN that ascends from the *j*th glomerulus). We do not know whether this PN–IN feedback is excitatory, but assume it to be so in this study. The model, however, can be used to explore the behavior of the network if we assume this feedback to be inhibitory. We also assume that the *j*th IN inhibits all the other INs but only inhibits the *j*th PN. Once the properties of this network are understood, the potential function of other classes of INs can be investigated.

In summary, our architecture centers around the assumption that each glomerulus is defined by a group of ORNs that excite a particular IN which we will henceforth refer to as originating from that glomerulus. This IN then forms an inhibitory–excitatory feedback loop with its associated PN. The INs each inhibit one another, although not themselves. Each PN fires because self-excitation (or, equivalently, excitation from sources not explicitly identified in the model) is disinhibited by inhibition of the IN synapsing with the PN in question [as suggested from the empirical studies of Christensen *et al.* (1993); see also Av-Ron and Rospars (1995)].

Time delays are included in our model so that the activity of an IN originating from a particular glomerulus affects INs originating from neighboring glomeruli sooner than INs originating from non-neighboring glomeruli. Topologically we assume that glomeruli are arranged in a circle (i.e. each has two nearest neighbors, which for glomerulus 1 are glomerulus *n* and glomerulus 2) and that they are not all necessarily connected to one another. This assumption of a circular arrangement appears to be supported by empirical observations (Rospars, 1983; Arnold *et al.*, 1985; Rospar and Hildebrand, 1992). Finally, we assume that ORNs can be categorized into one of *n* classes, and that all ORNs of the *j*th class arborize in the *j*th glomerulus and synapse with the *j*th IN. In reality, the categorization of ORNs is not as clean as originally thought (see Akers and Getz, 1992), but the assumption that ORNs synapsing within the same

glomerulus should at least be similar appears to be the most reasonable assumption in the absence of evidence to the contrary (Rospars and Fort, 1994).

Antennal lobe equations

The antennal lobe equations are obtained by restricting the synapse weights in the general set of network equations (equation 3 in Appendix A) to be zero if the neurons in question do not connect with one another, positive if the connections are excitatory and negative if the connections are inhibitory. We also treat the ORN spiking rates as given constant inputs. This allows us to study the dynamic properties of the antennal lobe network without the confounding influence of phaso-tonic (dynamic) ORN inputs. Once the computational properties of the antennal lobe network are better understood, then the effects of more realistic ORN input can be studied using dynamics models of ORN responses (e.g. see Av-Ron and Rospars, 1995; Av-Ron and Vibert, 1996) to constant and temporally varying stimuli using available data (Lemon and Getz, 1997) as a basis for developing the ORN component of the model.

The model includes background firing rates for each neuron. These rates could be due to self-excitation or unaccounted input from neurons not included in the architecture presented in Figure 1 [e.g. certain ventral unpaired median neurons such as VUMmx1 have been implicated in sending information from the subesophogeal ganglion to various parts of the insect brain including the antennal lobes—e.g. see Hammer and Menzel (1995)], or related to threshold effects (as discussed in Appendix A).

Receptor input

Olfactory ORNs in insects range from those specialized to respond to single critical compounds (pheromone receptor neurons) to those responding to several classes of compounds (for reviews see Masson and Mustaparta, 1990; Smith and Getz, 1994; Hildebrand and Shepherd, 1997). Most, however, respond to large suites of compounds (Sass, 1978; Selzer, 1984; Fujimura *et al.*, 1991; Akers and Getz, 1992, 1993; Getz and Akers, 1993, 1997) and exhibit nonlinear responses with respect to both concentration gradients and pure compounds versus mixtures of compounds (Getz and Akers, 1995), as well as phaso-tonic profiles over stimulus intervals of varying lengths (Lemon and Getz, 1997). Recently, Malaka *et al.* (1995) constructed response surfaces for pure compounds and mixtures of these compounds, using honey bee olfactory receptor data obtained by Akers and Getz (1993), and used these surfaces as input to neural networks performing olfactory computations (Malaka *et al.*, 1996).

The tuning and temporal properties of ORNs have been studied, even modeled (Linster and Dreyfus, 1996; Linster and Masson, 1996), in some detail. In our analysis we reiterate that we do not include a dynamic model of the ORNs to capture their phaso-tonic response to stimulation (Akers and Getz, 1992; Lemon and Getz, 1997), nor do we include details of the nonlinearities [inhibitions and synergisms (see Getz and Akers, 1995)] associated with the response of olfactory ORNs to mixtures compared with their response to pure odorants. Rather, because our focus is on how certain antennal lobe architectural features may determine antennal lobe olfactory processing qualities, we model the response of the ORNs to constant olfactory stimuli of fixed duration in terms of constant spiking rates.

Network output

The output from the network is the responses of the PNs that will vary depending on the particular input stimulus, as well as the values of the network parameters. These values include the dimension of the model itself, activation, response decay, transmission delay and synapse weighting parameters, as well background firing rates. As already mentioned, we will not consider stimuli with spatial heterogeneity, although this can be incorporated into the model as has been done in the context of simpler network representations of antennal lobe computations (Malaka *et al.*, 1996). Even though our stimuli have no temporal component other than being switched off at the end of the stimulus interval, however, we still need to deal with temporal structure in the output.

If a uniform stimulus is applied across the antenna for, say, 200 ms, then in the honey bee and cockroach we know that the general olfactory receptor neurons reach maximum firing rate within 50 ms and begin to adapt after ~150 ms (Akers and Getz, 1992; Lemon and Getz, 1997). The receptor neurons rapidly return to background firing rates after the stimulus is removed. Thus a 100 ms square pulse represents a good approximation to the critical processing period for odors of moderate concentration (Getz and Akers, 1997). The PNs, however, continue to respond for several hundred milliseconds after the stimulus has been removed (Laurent *et al.*, 1996; Lemon and Getz, 1999). Thus, we will consider the response of the PNs for the duration of a 100 ms input pulse in the ORNs and for 300 ms beyond the offset of this input pulse.

Simple ways to compare two 400 ms output response profiles is to split them into bins (say 50 ms intervals), calculate average firing rates over each of these eight subintervals in question and treat the eight resulting numbers as an eight-dimensional vector (Figure 2). The similarity of the quality of the odors coded by two output patterns can then be measured using the inner product between the vectors (of average firing rates over eight 50 ms bins) associated with the patterns in question. By interpreting the direction of the vectors in our eight-dimensional space as coding for odor quality (Figure 2), and the magnitude of the vectors as coding for concentration (see Getz and Chapman, 1987), we can train the network (i.e. progressively update the values of the network parameters using a genetic algorithm—see Appendix B) to optimize the network's ability to recognize

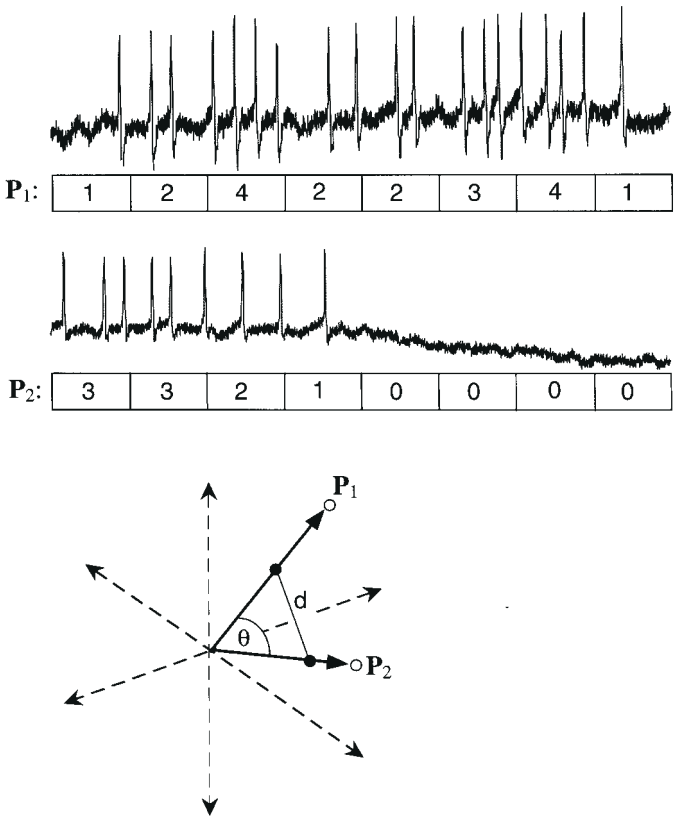

Figure 2 The spike train output from two different projection neurons over a 400 ms time interval is depicted together with corresponding output vectors P_i, $i = 1, 2$, obtained by dividing the time interval into eight 50 ms bins and then recording the number of spikes in each time bin. (Note that in the network model we do not produce the spikes themselves but only the probability of firing over one 5 ms time iteration of the model, from which ten consecutive values can be used to obtain the average rate over each 50 ms time bin.) The eight values associated with each output vector then represents a point in eight-dimensional Euclidean vector space. In this figure, for clarity, we depict the situation in three- rather than eight-dimensional space. The open circles represent the points connected to the origin by the vectors they represent. The angle θ between the two vectors is one measure of the similarity of the odor quality they represent. The solid circles represent the normalized vectors ($P_i/\|P_i\|$) and the distance $d = (\|(P_1/\|P_1\|) - (P_2/\|P_2\|\|)$ is another measure of the similarity of the odor quality. [It is the one as used to define the performance indices Q and D in expressions (7) and (8) in the Appendix B.]

odor quality independent of concentration and discriminate among odors of different quality (see Appendix B for more details).

In more sophisticated approaches, we can feed the PN output into a 'classifier network' of some kind (i.e. the output becomes input into another network). From a biological perspective, this classifier network represents a higher order memory center, such as the mushroom bodies of the insect protocerebrum (reviewed by Menzel *et al.*, 1991; also see Laurent *et al.*, 1996). In this study, however, we define two vector-based measures of performance with respect to a given set of stimuli representing several different odors each of which can be presented at one of three different concentrations (see Appendix B for details).

The first performance index, Q (defined by equation 7 in Appendix B), is a measure of the average distance between stimuli of the same odor quality, and can thus be regarded as a quality voracity performance index. From the definition of Q it follows that the voracity of coding for quality increases or improves as the measure Q decreases in value. The second performance index, D (defined by equation 8 in Appendix B), is a measure of the average distance between stimuli of different odor qualities (Figure 2). It can thus be regarded as a discrimination performance index. From the definition of D it follows that the ability of the network to discriminate among odors improves as the measure D increases in value.

From these two measures a third measure $R = D/Q$ can be defined (see equation 9 in Appendix B) that permits the performance of the network to be simultaneously measured with respect to both veracity and discriminability of quality coding. From the definition of R it follows that the overall performance of the network generally improves as the value of the measure R increases. Note, from the definition of these measures in Appendix B, the network cannot begin to distinguish between *odors of different qualities at the same concentration* and *odors of the same quality at different concentrations* unless $R > 1$, and cannot perform very well unless $R >> 1$.

Three and six odorant simulations

For all the simulations reported in this paper, the dimension of the net (i.e. the number of glomeruli and output neurons) is $n = 6$ and the number of types of receptor neurons is also 6 (cf. Figure 1), with response values defined by equations (6) (Appendix B). In our first set of simulations, we confined our attention to three-dimensional stimuli of the form $S = (C_1,C_2,C_3)$, where C_i is a logarithmically transformed value of the actual concentration of odorant i. Because empirical data indicate that the average rate of response of many ORNs to odorants is proportional to the logarithm of concentration between threshold and saturation levels (e.g. see Fujimura *et al.*, 1991), the odors C_i can be scaled in future studies using real data. To keep things simple, we assume that the ORNs switch on and off instantaneously and respond tonically to constant stimuli. Further, in our first set of simulations we consider two classes of ORNs: 'linear specialist', which respond to only one odor (namely, the ith ORN of this type responds to odorant i at a firing rate C_i), and 'linear differencers', which respond only to the presence of two odorants (namely, the ijth ORN of this type responds to odorants i and j at a firing rate $|C_i - C_j|$—see Appendix C). Thus the second class of ORNs exhibit inhibition to mixtures containing the two odorants in question, a phenomenon that is widespread in insects (Getz and Akers, 1995) and also crustaceans (Derby *et al.*, 1989).

The analyses of the performance of the network involved training the network using a genetic algorithm (Appendix B) to classify and discriminate among stimuli by setting the concentrations of the odorants C_i, $i = 1, 2, 3$, in the stimulus $S = (C_1,C_2,C_3)$ to be $C_i = C^0 - \Delta C$, C^0 or $C^0 + \Delta C$. Thus the stimuli are all essentially characterized in terms of log concentration rate parameters C^0 and ΔC that translate either directly (linear specialist ORNs) or indirectly (linear differencer ORNs) into ORN response rates (see equations (11) in Appendix C for more details). Thus the stimuli ($C^0 - \Delta C$, $C^0 - \Delta C$,0) and ($C^0 + \Delta C$, $C^0 + \Delta C$,0) represent the same odor (an equicomponent mixture of odorants 1 and 2) at a high and low concentration, while the stimuli ($C^0 - \Delta C$, $C^0 + \Delta C$,0) and ($C^0 + \Delta C$, $C^0 - \Delta C$,0) represent blends of the same two odorants but in different proportions and therefore of different quality.

A more challenging problem for the network than classifying and discrimination among stimuli consisting of three components is to one involving stimuli consisting of six components [i.e. stimuli of the form $S = (C_1,C_2, C_3,C_4,C_5,C_6)$—see Appendix D]. As in the three odorant case, we defined pure odorant stimuli at three different concentrations in terms of response rate parameters C^0 and ΔC and blends of these stimuli using these same two concentration parameters (Appendix D). For comparative purposes, we retained six classes of ORNs but went beyond the elementary case of defining six specialist neurons (one for each odorant) by rather defining three 'binary specialists' (each responding now to two rather than one odorant) and three 'binary differencers' (each responding to the difference between two pairs of binary odors). In this case, we no longer have receptor neurons that specialize on any one single odorant (Appendix D).

Parameters and notational issues

The symbols and meaning of the various parameters used in the model and the values used in the analysis are listed in Table 1. We used a genetic algorithm to find the three sets of IN–IN synapse parameters that optimize (at least in some local sense) the quality performance index, Q, the discrimination performance index, D, or the ratio index $R = D/Q$ when the remaining parameters in the network have the values indicated in Table 1. To avoid confusion in discussing our results, we use the following notation to describe the solutions to these three separate optimization problems. First, for the given set of stimuli, we use $Q(P)$, $D(P)$ and $R = R(P)$ to denote the values of the measures Q, D and R, (equations 7–9 respectively in Appendix B) with respect to a given set P of parameter values. Second, we include the time variable t explicitly when we want to emphasize that the solution is the best one found by our genetic (i.e. evolutionary) algorithm up to generation time t; for example, $R(P_R(t))$ is the best solution obtained to the problem of optimizating the ratio measure after the genetic algorithm has run for t generations, while $R(P_D(t))$ is the actual value of the performance measure R for the parameter set that is the best solution to this problem of optimizing the discrimination measure D after t generations. Third, we use the notation P_Q^*, P_D^* and P_R^* to denote the candidate optimal parameter sets respectively as solutions to optimizing the measures Q, D and R. Note our solutions are only candidates to solving the optimization problem because they may correspond to local rather than global optima. Also, they are only numerical approximations at that. Fourth, we use the notation Q^*, D^* and R^* to denote the candidate optimal values of these respective measures; that is, $R(P_R(t)) \to R^*$ as $t \to \infty$, provided the solution does not get trapped by a local optimum. More loosely, however, we use this notation to denote the best solution and values we find within the time constraints we impose upon the genetic algorithm. Fifth, the triplets (Q^*, $D(P_Q^*)$, $R(P_Q^*)$), ($Q(P_D^*)$, D^*, $R(P_D^*)$) and ($Q(P_R^*)$, $D(P_R^*)$, R^*) (where $Q^* = Q(P_Q^*)$, etc.) are the values of the three measures in question when the criteria Q, D and R respectively are optimized. Finally, at the risk of laboring the point, we use the triplet (Q^*,$Q(P_D^*)$,$Q(P_R^*)$) to denote all the values of the performance measure Q when evaluated respectively for parameter sets P_Q^*, P_D^* and P_R^*; and, similarly, for the triplets ($D(P_Q^*)$,D^*,$D(P_R^*)$) and ($R(P_Q^*)$, $R(P_D^*)$,R^*).

Note that our optimization solutions are all in the context of the set of stimuli used to generate the performance measure Q, D and R (as defined in expressions 7 and 9 in Appendix B). This dependence is consonant both with learning over intragenerational time scales and with natural selection over intergenerational time scales, because organisms should develop or evolve to maximize their ability to discriminate among stimuli that they encounter during their life times. Also note that each case (i.e. selection of parameters that are *a priori* fixed) requires the genetic algorithm to be rerun to obtain the optimal solution for the case in question.

Results

Evolution over time

To address the question of how well the genetic algorithm converges on an optimal solution, we ran several simulations for many tens of thousands of generations. In each of these simulations, we used the set of parameter values listed in Table 1, but the 100 individuals for the initial population in each simulation were picked at random (i.e. for each individual, the weights w_{ij} were randomly assigned one of their four possible values). We found that the system converged much more rapidly for high ($w_j = 1.2$, $j = 1, \ldots, 6$) compared with low ($w_j = 0.4$, $j = 1, \ldots, 6$) PN–IN feedback synapse values (Table 2). Because 5000 generations usually provided enough time for our genetic algorithm to achieve close to 90% of the value obtained after 100 000 generations, to save computational time we restricted our simulations to 5000 generations (Table 2).

Table 1 Fixed and optimized values of parameters used to carry out simulations

Parameter name	Symbol	Equation	Value used
Time	t	(4)	1 unit = 5 ms
Dimension of net	n	(4)	6 (number of glomeruli)
Number of stimuli	M	(7–8)	3 or 7 for 3 odorant case[1] 6 or 22 for 6 odorant case
Activation function slope	$\beta_1 \geq 0$ and $\beta_2 \geq 0$	(2)	0.3
Activation function locations	θ_1 and θ_2	(2)	0.0
Memory parameters	$\mu_j \geq 0$ and $\overline{\mu}_j \geq 0$, $j = 1, \ldots, 6$	(4)	0.4
IN–IN delay parameters	$\delta_{jk} \geq 0$, $j, k = 1, \ldots, 6$	(4)	1 for $\lvert j-k \rvert = 1$ modulo 6 2 for $\lvert j-k \rvert = 2$ modulo 6 0 otherwise[2]
IN–PN delay parameters	$\hat{\delta}_j \geq 0$, $j = 1, \ldots, 6$	(4)	0
PN–IN delay parameters	$\delta_j \geq 0$, $j = 1, \ldots, 6$	(4)	0
RN–IN feedforward synapse strengths	$\tilde{w}_{jj} \geq 0$, $j = 1, \ldots, 6$[3]	(4)	1
IN–PN feedforwardsynapse strengths	$\overline{w}_k \leq 0$, $k = 1, \ldots, 6$	(4)	4.5
PN–IN feedback synapse strengths	$\hat{w}_j \geq 0$, $j = 1, \ldots, 6$	(4)	0.4 or 1.2
IN–IN connection synapse strengths	$w_{ij} \leq 0$, $i, j = 1, \ldots, 6$	(4)	values optimized using genetic algorithm (see Table 3)[4]
IN self-activation rate	$l_j \geq 0$, $j, k = 1, \ldots, 6$	(4)	1
PN self activation rate	$\overline{l}_k \geq 0$, $j, k = 1, \ldots, 6$	(4)	$\overline{w}_k/2 = 25$[4]
IN initial conditions	$y_j(0) \geq 0$, $j = 1, \ldots, 6$	(4)	0.5
PN initial conditions	$z_j(0) \geq 0$, $k = 1, \ldots, 6$	(4)	0.5

[1]The first value pertains to performance measure (7) and the second to performance measure (8).

[2]These values are based on the assumption that, topologically, the six glomeruli are arranged in a circle and that each IN identified with each glomerulus affects its two nearest neighboring INs with a 10 ms time-delay and its two next nearest neighboring INs with a 15 ms time-delay, but does not synapse with the 5th IN that is furthest from it. Note that a circular arrangement of the glomeruli in that antennal lobe has empirical support (Arnold *et al*., 1985; Rospars and Hildebrand, 1992).

[3]We only consider the case of one input synapsing with each glomerulus so that w_{jj} does not exist for $i \neq j$. The single jth input neuron represented here can be thought of as the aggregated input across all RNs of class], which is a reasonable simplification if features relating to the spatial distribution of receptor neurons along the antennae are not considered. When spatial heterogeneity is included in the stimuli then this assumption must be dispensed with and the full set of receptor inputs considered (cf. Malaka *et al.*, 1996).

[4]The values are represented by a two-bit binary word, so that each weight is able to assume one of the values –3, –2, –1 and 0. The level of resolution in selecting values for these weights can of course be increased by letting each weight be represented by a four- or eight-bit word. Since each IN is only connected to its four nearest neighbors and not to itself, we set $w_{ij} = 0$ when $\lvert i-j \rvert = 2$ modulo 6, and set $w_{jj} = 0$, $i, j = 1, \ldots, 6$. Thus, the actual number of possible parameter sets is still a large number (namely, $4^{24} \approx 2.81 \times 10^{14}$), considering the two-bit level of resolution used here.This value was selected so that initially the PNs have a background firing rate that can either be augmented (depolarized) or inhibited (hyperpolarized) in response to an external stimulus.

Also evident from Table 2 is the fact that improvements in ratio R ($PR(t)$) over time were not due to a steady improvement in both quality verity Q (t) and stimulus discrimination D (t), but sometimes corresponded to decreased performance in one of these measures that was more than compensated for by an increase in performance of the other measure. Also, in the low PN–IN feedback case ($w_j = 0.4$, $j = 1, \ldots, 6$) improvements in the ratio R ($PR(t)$) were due more to improvements in stimulus discrimination D (t) than to improvements in quality verity Q (t), while for the high PN–IN feedback case ($w_j = 1.2$, $j = 1, \ldots, 6$) most of the improvements in the ratio R ($PR(t)$) were due a dramatic improvement in quality verity Q (t) over time (Table 2). Thus, compared with the low PN–IN feedback case, the high PN–IN feedback case produced a quality code that was more than three times as good (2.5 is more than three times smaller than 8.35), but a discrimination code that was less than twice as good (12.66 is less than twice as large as 6.9). Combining these two results, the ratio R^* for the high PN–IN feedback case is more than six times larger than the ratio R^* for the low PN–IN feedback case. One of the reasons for this difference (as we shall see in Figure 4 below once we present the dynamic responses of the PNs to the three odorant stimuli) is that in the low PN–IN feedback case the PNs relax to a stimulus-independent state after the stimulus is removed, while in the high PN–IN feedback case after the stimulus is removed the PNs remain in a state that is close to the state they are driven to in the presence of the stimulus.

In our simulations we found that some of the solutions appeared to get temporarily trapped by local minimum solutions for varying lengths of time. To deal with this problem, while still retaining a sense of the effects that local

Table 2 A typical run of the genetic algorithm for the solution trajectory of the various performance measures (see expressions 7–9 in Appendix B) using the standard set of parameters and the two indicated PN–IN feedback values w_j, $j = 1,, \ldots, 6$

Generation[1] (time t)	R ($P_R(t)$)	$Q(P_R(t))$ ($\times 10^{-3}$)	$D(P_R(t))$ ($\times 10^{-2}$)
$w_j = 0.4$			
1	4.08	6.87	2.80
2	4.90	6.23	3.05
3	5.11	6.08	3.10
12	5.35	6.14	3.28
32	5.40	6.02	3.25
49	5.52	6.33	3.50
310	5.60	6.02	3.37
421	5.78	6.02	3.48
1956	6.43	6.34	4.07
2303	6.53	6.48	4.23
3099	6.54	6.39	4.18
3424	6.55	6.59	4.31
3707	6.71	6.46	4.33
3763	7.02	6.56	4.60
4364	7.06	6.94	4.90
4612	7.13	6.67	4.75
5060	7.24	7.26	5.26
5087	7.33	6.78	4.97
5527	7.33	7.10	5.20
5733	7.50	6.94	5.21
6082	7.52	7.47	5.62
6128	7.53	7.09	5.34
6505	7.55	7.14	5.39
6645	7.61	7.51	5.72
6979	7.69	7.67	5.90
7412	7.71	7.71	5.94
7503	7.75	7.40	5.73
8683	7.81	7.73	6.04
9065	7.95	7.96	6.32
14 921	8.03	7.50	6.03
15 284	8.07	7.42	5.99
17 457	8.10	7.85	6.36
22 673	8.19	8.08	6.61
92 670	8.25	8.41	6.93
111 631	8.28	8.35	6.91
$w_j = 1.2$			
1	3.07	32.51	9.98
2	6.99	16.16	11.29
4	7.16	13.65	9.77
12	9.26	13.34	12.35
19	10.87	8.41	9.14
41	19.88	5.89	11.68
166	22.27	5.66	12.61
299	26.01	4.54	11.81
380	26.54	4.49	11.92
431	33.65	3.76	12.66
460	34.12	3.49	11.92
558	40.65	3.13	12.73
668	41.54	3.08	12.81
699	44.59	2.67	11.92
790	48.22	2.47	11.89
809	50.44	2.55	12.86
1069	50.68	2.54	12.87
1304	51.01	2.53	12.92
1468	51.30	2.52	12.91
2616	51.74	2.50	12.94

[1]At every recorded point in time the value of R , defined by formulation (9) (Appendix B) and obtained from the genetic algorithm, exceeds all previous values. These values are plotted along with the generation at which this new maximum value was obtained. The corresponding values of the performance measures Q and D are also evaluated for the same 'best parameter set to date', enabling us to assess to what extent improvements in R were due to improved quality coding Q (smaller values are better) or improved discrimination D (larger values are better). Note that for the second case the value at $t = 2616$ was not exceeded by the time the simulation ceased after more than 100 000 generations.

minima might have on a single net in an adaptive learning situation, we report in the analyses below the average values of our various performance measures for trajectories starting from five different randomly selected initial conditions. These five sets of 100 initial network configurations were used in all related simulations which, as mentioned above, were each run for only 5000 generations.

Effects of concentration

In the context of trying to understand the role of the different parameters on the performance of the network, we began by examining the extent to which a relatively large value of ΔC (recall the highest and lowest concentrations used as stimuli are $C^+ = C^0 + \Delta C$ and $C^- = C^0 - \Delta C$ respectively) degrades the performance of the network (Figure 3A) by setting $\Delta C = 1$ and allowing the value of C^0 to take on integer values from 2 to 6 (cf. the horizontal axes in Figure 3A–D). As expected, the performance measure R^* improves steadily from ~23 to 199 as C^0 increases from 2 to 6 and dominates the values of the ratios R (P_Q*) and R (P_D*) respectively obtained by optimizing only with respect to the quality performance measure, Q , and then only with respect to the discrimination performance measure, D. We also generated values of Q^*, D^* and R^* with respect to C^0 for the cases $\Delta C = 0.5$, 1, 2 and 3 (Figure 3B–D). In general the discrimination performance measure, D^* (Figure 3C), was indifferent to the value of C^0 and ΔC, except for low values of C^0 ($C^0 = 2$). As expected, however, the quality performance measure was degraded (i.e. the value increased; Figure 3B), and thus the overall performance measure, R^*, was also degraded (i.e. the value decreased; Figure 3D) with the value of the ratio $\Delta C/C^0$.

Activation and memory parameters

Next we examined the effect that the values of the activation function steepness parameters, β_1 and β_2 (i.e. how rapidly neurons switch from their off to on state as the level of membrane depolarization increases—see equation 2 in

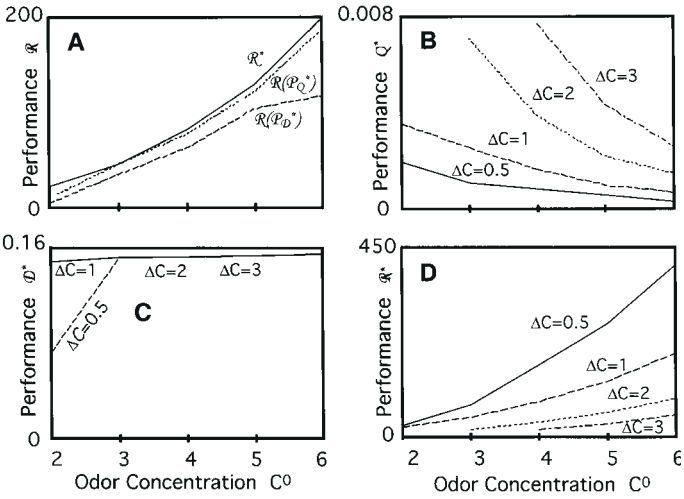

Figure 3 The value of the performance measures Q, D and R (see expressions 7–9 in Appendix B) are plotted for the medium concentration level ranging from C^0 = 2–6 and for the remaining parameter values specified in Table 1. In **(A)**, $\Delta C = 1$ and the values of the performance ratio R (expression 9) are plotted for the parameter sets P_Q*, P_D* and P_R* that are the candidate solutions to problems (7–9). In **(B–D)** respectively the quality Q*, discrimination D* and ratio R* performance values are plotted for the four cases, ΔC = 0.5, 1, 2 and 3. (Note that for the larger values of ΔC the plots begin at larger values of C^0 to satisfy the requirement that $C^0 - \Delta C > 0$.)

Appendix A and Table 1), have on the optimal values Q*, D* and R* (Figure 4A–C) for different values of C^0 (ΔC = 1). Specifically, we compared the increasingly nonlinear activation functions $\beta_1 = \beta_2$ = 0.3, 0.5 and 0.8. All three measures, Q*, D* and R*, improve with increasing nonlinearity in that activation function, and identification of quality becomes almost perfect (Q* close to zero; Figure 3A) for the case $\beta_1 = \beta_2$ = 0.8 when the ratio $\Delta C/C^0$ is one-quarter or less (i.e. C^0 = 4). Since the discrimination performance measure, D*, is insensitive to this ratio (except for the one slightly anomalous point $\beta_1 = \beta_2$ = 0.3 and C^0 = 3; Figure 4B), the overall performance measure, R*, is very large (>14 000) for the case $\beta_1 = \beta_2$ = 0.8 (Figure 4C).

We also examined the effect of the values of the neuron decay (memory) parameters μ_j and $\overline{\mu}_j$ (i.e. how rapidly activity in neurons ceases once stimulation is removed—see equation 4 in Appendix A and Table 1) on the measures (Q (P_R*),D (P_R*),R*) by evaluating these measures for the cases $\mu_j = \overline{\mu}_j$ = 0.1, 0.2, 0.3, 0.4 and 0.5, j = 1, . . . , 5 (Figure 4D–F). Discrimination, D*, improved (increase in value of the performance measure) with increasing values of the decay parameters (Figure 4E), while quality assessment only improved (decrease in value) for the decay parameter increasing to $\mu_j = \overline{\mu}_j$ = 0.3, held steady at $\mu_j = \overline{\mu}_j$ = 0.4 and deteriorated for $\mu_j = \overline{\mu}_j$ = 0.5 (Figure 4D). The optimal value

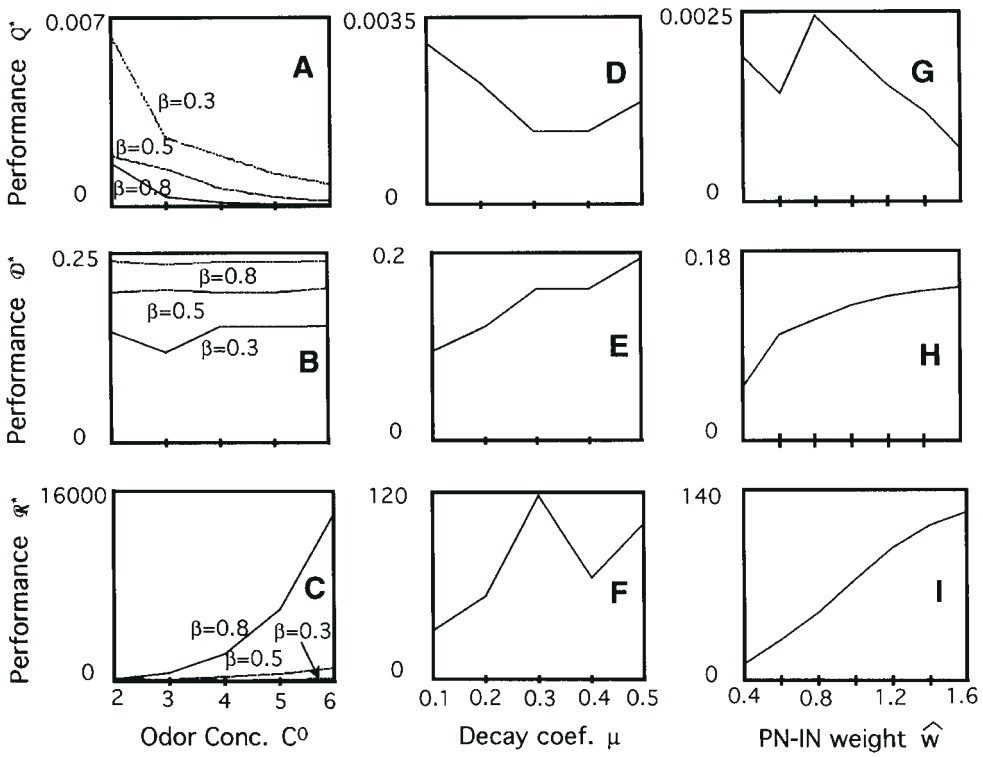

Figure 4 The candidate optimal values of the performance measures Q*, D* and R* (defined in expressions 7–9 in Appendix B) are plotted for the standard set of parameter values specified in Table 1, except for changes in selected parameter values as labeled on the horizontal axis. Specifically, the values of the performance measures are plotted for β = 0.3, 0.5 and 0.8 in terms of C^0 ranging from 2 to 6 with ΔC = 1 **(A–C)**, for fixed β = 0.3 and concentrations parameters (C^0,ΔC) = (4,1) in terms of the decay coefficients ranging from 0.1 to 0.5 **(D–F)**, and in terms of the PN–IN feedback coefficients w ranging from 0.4 to 1.6 **(G–H)**.

of the ratio R^* also improved with increasing values of μ_j and $\overline{\mu}_j$ until the value $\mu_j = \overline{\mu}_j = 0.3$ was obtained, but then decreased for $\mu_j = \overline{\mu}_j = 0.4$ and increased again for to $\mu_j = \overline{\mu}_j = 0.5$ (Figure 4F).

Projection neuron feedback parameters

Finally, we examined how that values of the PN–IN feedback synapse parameters $\hat{w}_j, j = 1, \ldots, 6$ (see equation 4 in Appendix A and Table 1), influenced the values of performance measures Q, D and R. In particular, we analyzed the cases $\hat{w}_j = 0.4, 0.6, 0.8, 1.0, 1.2, 1.4$ and 1.6 for $j = 1, \ldots, 6$ (increasing values imply strengthened feedback effects), using our standard set of parameter values (Table 1) and the values $(C^0,\Delta C) = (4,1)$ (Figure 4G–I). The optimal discrimination and ratio values, D^* (Figure 4H) and R^* (Figure 4I) respectively, improved (i.e. increased) with increasing feedback, while the optimal quality Q^* (Figure 4G) only improved (i.e. decreased) over the higher values of the PN–IN feedback synapse weights $\hat{w}_j, j = 1, \ldots, 6$.

In Table 3 we list the final set of IN–IN synapse values w_{ij}, $i,j = 1, \ldots, 6$ (see equation 4 in Appendix A), after optimizing R^* for the standard set of parameters (Table 1 with the PN–IN feedback coefficients having the values $\hat{w}_j = 1.2, j = 1, \ldots, 6$) and odor input parameters $(C^0,\Delta C) = (4,1)$. Note the values w_{ij}, $i,j = 1, \ldots, 6$, are not forced to be symmetric (i.e. w_{ij} is not necessarily equal to w_{ji}), as is the case for a standard Hopfield recurrent network (Haykin, 1994, p. 557): there is no reason why these synapse values should be symmetric if allowed to evolve in the absence of a constraint that enforces such symmetry (the symmetry constraint facilitates theoretical investigations of the stability properties of the network but is not needed in context of the numerical simulations reported here).

We also provide examples of the output in response to various input stimuli for the same set of PN–IN feedback synapse parameters, $\hat{w}_j = 1.2, j = 1, \ldots, 6$ (Figure 5A–C), and compare this to the case where the PN–IN feedback coefficients are $\hat{w}_j = 0.4$, $j = 1, \ldots, 6$ (Figure 5D–I). Comparing panels A–C with panels D–F in Figure 5, it is clear that for the set of network parameters considered here, the high feedback has the effect of rapidly stabilizing the output compared with the low feedback. Further, with high feedback, PN activity stabilizes at stimulus-dependent equilibria, while with low feedback it stabilizes at a stimulus-independent equilibrium. Thus, in the high-feedback case, PN equilibrium values can represent the code, while in the low-feedback case only the 0–150 ms PN transient can represent the code. In the latter case, the PN transient has the same pattern at low, medium and high concentrations (Figure 5G–I), although the amplitudes of the PN transients are slightly more extreme in the case of the high (5I) compared with the low (5G) concentration stimulus.

As we noted earlier, and is evident from Figure 5A–I, each of the PNs has an initial spiking rate that is around the middle of its firing range scaled so the maximum corresponds to a value of 1 (this is obtained by setting the corresponding PN membrane activation potential to $z_k(0) = 0.5$, $k = 1, \ldots, 6$—see Appendix B for details). For the low PN–IN feedback case $\hat{w}_j = 0.4$, $j = 1, \ldots, 6$, the system appears to have a single relaxed state (i.e. stable equilibrium), and we would expect that the system would be in this state prior to stimulation. As the network evolves, this unstimulated relaxed state will change from stimulus to stimulus so that its value is not known *a priori*. In this case, this relaxed state cannot be used as a universal initial condition to implement the genetic algorithm. To get around this problem in our simulations, we selected the intermediate values $z_k(0) = 0.5$, $k = 1, \ldots, 6$ as initial conditions for all PNs throughout the course of the genetic algorithm. Further, if the feedback has the relatively high value $\hat{w}_j = 1.2, j = 1, \ldots, 6$, the system relaxes after removal of the stimulus to states that are stimulus dependent (and appear to be relatively close to the states to which the system is driven by the stimulus being applied for the first 100 ms of the 400 ms evaluation interval). Thus, if the system starts out in a relaxed state after application of a particular stimulus and a new stimulus is applied for a sufficiently short interval of time, the system will not move far from its initial state and relax back to that same state. This dynamic behavior implies that if codes are to persist beyond the application of stimuli, each stimulus must be applied for a sufficiently long period of time to enable the network to be driven to a new region of its state space. Then after removal of the stimulus in question the network is able to relax to a state that is uniquely determined by this new stimulus (i.e. independent of the initial condition). On the other hand, if codes are contained in the initial transient, the network needs to be reset to the same initial state prior to stimulation through a priming mechanism that is internally generated. One such mechanism could be synchronizing oscillations that have been observed in the insect antennal lobes

Table 3 The values of the IN–IN feedback synapses parameters w_{ij}, $i, j = 1, \ldots, 6$ obtained after maximizing the performance ratio, R, with respect to the standard set of parameter values and stimulus concentrations $(C^0,\Delta C) = (4,1)$ (i.e. parameter set $P_R{}^*$ and solution R^*)[1]

IN_j	$j = 1$	$j = 2$	$j = 3$	$j = 4$	$j = 5$	$j = 6$
$j = 1$	0[2]	2	1	0[3]	0	0
$j = 2$	0	0[2]	2	0	0[3]	3
$j = 3$	1	2	0[2]	2	0	
$j = 4$	0[3]	2	0	0[2]	1	2
$j = 5$	3	0[3]	1	2	0[2]	1
$j = 6$	3	3	0[3]	1	0	0[2]

[1]These values are not symmetric, as required for a standard Hopfield net (Haykin, 1994).

[2]These values are zero because the INs do not feedback on themselves.

[3]These values are zero because the INs only connect with their four nearest neighbors.

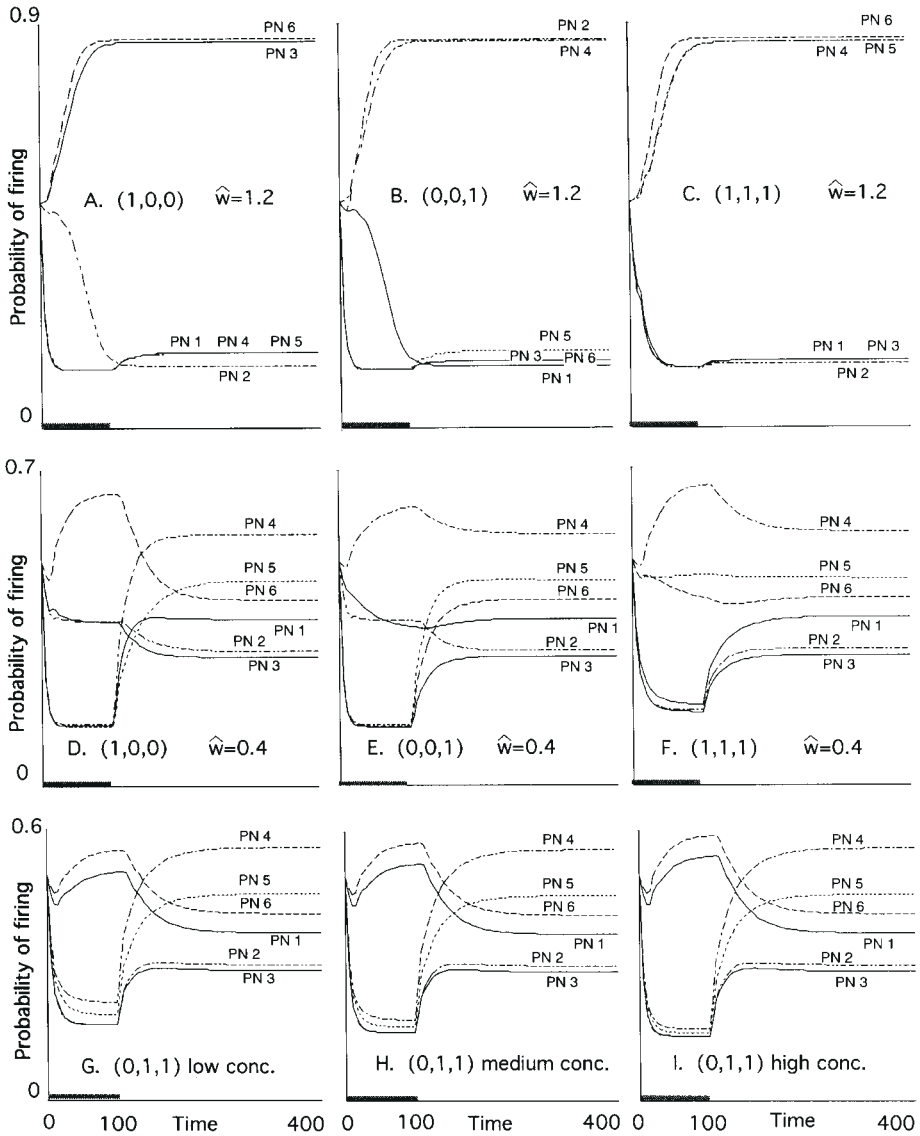

Figure 5 The output values of the six PNs are plotted over the 0–100 ms stimulus interval (thick gray line) and the subsequent 100–400 ms time interval for the PN–IN feedback synapse values $\hat{w}_j = 1.2, j = 1, \ldots, 6$ **(A–C)**, and $\hat{w}_j = 0.4, j = 1, \ldots, 6$ **(D–I)**. The remaining parameter values are specified in Table 1. The stimuli used are labeled in the panels, as are the concentrations used (low: $C^0 - \Delta C = 3$, medium: $C^0 = 4$ and high: $C^0 + \Delta C = 5$). The initial values are preset (Table 1), the transients over the interval [0,100 ms] are the system relaxing to the stable state corresponding to the forced system (forced by the labeled constant stimulus input), while the remaining component of the signal is the system relaxing to an unforced stable state (which is stimulus dependent in panels A–C and stimulus independent in panels D–I).

(Laurent and Davidowitz, 1994; Laurent *et al.*, 1996). Since we do not have any data on how the brain deals with this problem, as mentioned above, we have taken the neutral stance of setting all the INs and PNs to have initial values that produce intermediate spiking rates [i.e. $y(0) = z(0) = 0.5$ prior to the onset of a new stimulus—see Appendix B and equation (4)].

Six odorant simulations

Turning now to the simulations carried out for the six odorant case (see Appendix D), the first question we asked is how well the network performs over 5000 generations compared with the three odorant set of stimuli considered above. We carried out this comparison for the measures Q, D and R (equations 7–9 in Appendix B), using the standard set of parameters (Table 1) with $\Delta C = 1$, and for C^0 ranging over the integers 2 to 6 (Figure 6A–C). The ability of the network to produce a stable quality code (small Q^*; Figure 6A) was equally poor in both the three and six odorant cases when $C^0 = 2$ and comparably good in both cases when $C^0 = 5$ and 6. The quality coding, however, was not as good for the six-odorant stimuli as it was for the three-odorant stimuli when $C^0 = 3$ and 4. In fact, the network showed no improvement in quality coding for the six-odorant stimuli

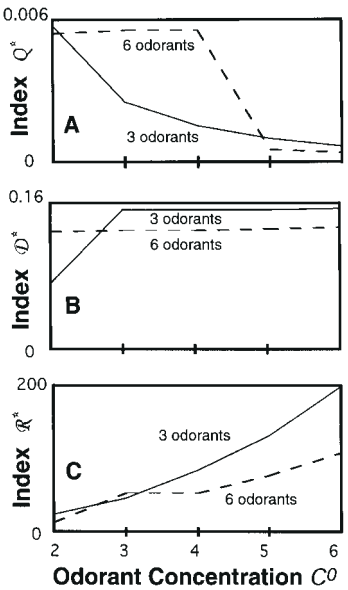

Figure 6 The optimal values of the performance measures Q^* **(A)**, D^* **(B)** and R^* **(C)** are plotted against the median concentration C^0 for the response of the network, with the parameters specified in Table 1 and $\Delta C = 1$, for the set of three (solid line) and six (broken line) odorant component stimuli respectively defined in equations (11a–c) (Appendix C) and (12a–c) (Appendix D).

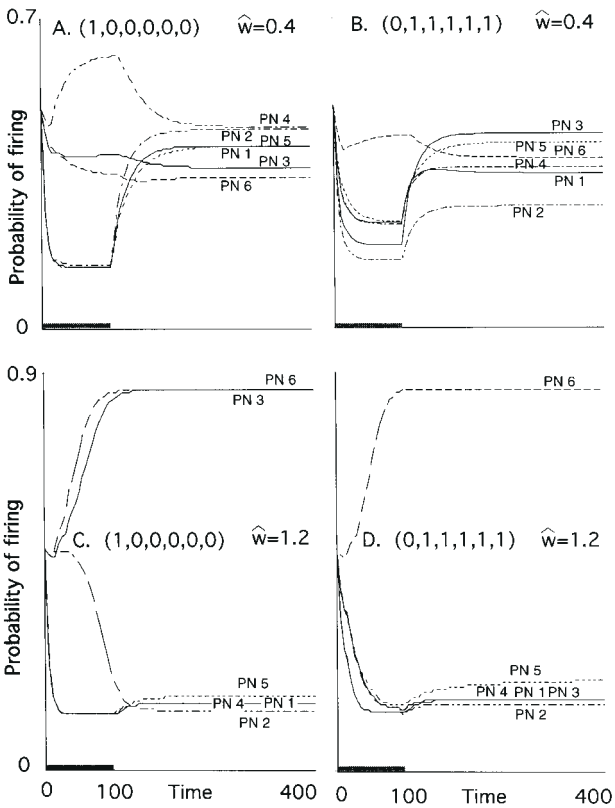

Figure 7 The output values of the six PNs are plotted, as in Figure 5, over the 0–100 ms stimulus interval (thick gray line) and the subsequent 100–400 ms time interval for the PN–IN feedback synapse values for the twocases $\hat{w_j} = 0.4$, $j = 1,\ldots, 6$ **(A, B)**, and $\hat{w_j} = 1.2$, $j = 1,\ldots, 6$ **(C, D)**. The remaining parameter values are specified in Table 1. The stimuli are all at concentration $C^0 = 4$ (medium) with the specific stimuli as labeled. The initial values are preset (Table 1), the transients over the interval [0,100 ms] are the system relaxing to the stable state corresponding to the forced system (forced by the stimulus as labeled), while the remaining component of the signal is the system relaxing to an unforced stable state (which, unlike the three-odorant case, is stimulus dependent for both moderate and strong PN–IN feedback; cf. Figure 5).

when $\Delta C/C^0$ fell from 1/2 to 1/3 and then to 1/4, but improved dramatically when $\Delta C/C^0$ fell to 1/5. Interestingly, the ability of the network to discriminate stimuli was better for the six-odorant than for the three-odorant stimuli at $C^0 = 2$, but the reverse was true for $C^0 = 3$, 4, 5 and 6 (Figure 6B). Also, from $C^0 = 3$ onwards, no improvement was evident in the ability of the network in either case to discriminate among odors.

The fact that the optimal quality performance measure, Q^*, is much more sensitive than the optimal discrimination performance measure, D^*, to the ratio $\Delta C/C^0$ is not surprising since a large ratio poses a challenge to quality coding, but does not affect discrimination, unless improvements in quality coding come at the expense of the networks discriminative abilities (as it does in the three-odorant but not the six-odorant case for the stimuli and receptor neurons under consideration). Note that the superior (larger) discriminative value D^* in the six-odorant case compared with the three-odorant case, when $C^0 = 2$, is not necessarily anomalous, since the receptor neurons defined by expressions (13) are not generalizations of the receptor neurons defined by expressions (10). If we set the odd or even odorants to zero (i.e. $C_2 = C_4 = C_6 = 0$ or $C_1 = C_3 = C_5 = 0$) then the ORNs defined by expressions (13) (Appendix D) exhibit excitatory rather than the inhibitory binary interactions that are evident in the ORNs defined by expressions (10) (Appendix C). Finally, the discrimination-to-quality ratio, R^*, improves steadily in both case as C^0 increases from 2 to 6 (Figure 6C), but the network performs almost twice as well in the three-odorant compared with the six-odorant set of stimuli when $C^0 = 6$.

We plotted selected outputs for the low ($\hat{w}_j = 0.4$, $j = 1, \ldots, 6$, Figure 7A,B) and high ($\hat{w}_j = 1.2$, $j = 1, \ldots, 6$, Figure 7C,D) PN–IN feedback cases (using the standard set of network parameters (Table 1) and stimulus parameters $(C^0,\Delta C) = (4,1)$. As with the three-odorant case, high feedback produces extreme PN output (close to 0 or close to 1), while low feedback allows the PNs to stabilize at intermediate values. Unlike the three-odorant low feedback case, however, the equilibria are now different for different odors in both the high and low feedback cases so that both the transient and equilibrium phases are able to contribute towards coding odor quality.

Discussion

With the constraints on the ranges of parameters in-

vestigated here, our results suggest that the performance of our network, as measured by the ratio R, (recall a good performance requires that $R >> 1$), is influenced at least threefold by the decay parameter μ ranging over 0.1–0.5 (Figure 4F), tenfold (an order of magnitude) by the PN–IN feedback synapse parameter ranging over 0.4–1.6 (Figure 4I) and an astonishing two orders of magnitude for the neuron activation function slope parameter β (equation 2 in Appendix A) ranging over 0.3–0.8 (Figure 4C). The performance of the network, however, is severly degraded as the concentration variation ratio $\Delta C/C^0$ is increased from 1/4 (the value that applies to all panels in Figure 4) towards 1 (see Figure 3). Thus the network, as it stands, has the potential to perform well for spatially homogeneous stimuli containing many more component odorants than the three and six odorants considered here (Figure 6), provided the value of the activation function slope parameter β is at least doubled from the value $\beta = 0.3$ used to generate all the plots in Figure 7.

Note that proportional changes in the input (i.e. in the logarithm of the concentration) do not produce proportional changes in the output (i.e. a linear response) because the neurons have nonlinear activation functions (threshold-like and saturation-like effects). Also the receptor neurons themselves are not all linear with respect to log-concentration of the components of the stimuli. The 'linear differencers' ORNs, for example, are dependent on the absolute value of the difference and thus will have a V-shaped response when, for example, the concentration of one of the two odorants to which these ORNs respond increases from less than to more than a given concentration of the other odorant to which they respond. Also, in the six-odor simulation case, none of the receptor neurons specializes on any one odorant, further confounding the quality and concentration coding task of the network.

Further, numerically intensive investigations are required to assess how well the system maintains its performance once the stimuli are given realistic temporal and spatial input structures. Of course, the performance can always be improved, at additional computational cost, by scaling up the dimensions of the network itself (i.e. increasing the number of glomeruli and associated number of ORNs, INs and PNs). The real issue is not whether the network can perform the computations required, but what the smallest network might be that will perform to some specified error rate for a given set of stimuli with associated temporal, spatial and concentration coefficients of variation. Further, the fact that the same type of ORNs are distributed across the antenna in a manner that is more uniform than random (Getz and Akers, 1994) also promotes the integration of temporal and spatial heterogeneity in the stimulus, assuming as we have that similar ORNs are more likely than random to arborize in the same glomerulus.

Perhaps one of the most interesting issues raised by our results relates to the possibility that the coding in real systems could either be in the initial transient, as is necessarily the case when the network equilibrium is independent of the stimuli (Figure 5D,E,F,H), or associated with the equilibria when the equilibria are stimulus dependent (Figure 5A,B,C). Of course, when the equilibrium is stimulus dependent, the coding could be in both the transient and equilibrium phases of the PN responses. Further, when the equilibrium is dependent only on the quality and not the concentration of the odor, as in the case of the high PN–IN feedback values ($\hat{w}_j = 1.2$, $j = 1, \ldots, 6$) for the three odor stimuli (Figure 5A–C) and all the six odor stimuli (Figure 7A–D), then the system has a true quality code over the range of concentrations used to train the network in optimizing the performance measure R (equation 9 in Appendix B). Even the transient phase for the low PN–IN feedback values ($\hat{w}_j = 0.4$, $j = 1, \ldots, 6$) in the three-odor stimuli case, however, provides a surprisingly robust quality code, despite the fact that once the stimulus is removed the system returns to a stimulus-independent equilibrium state. For example, the only difference between the transients for the odor stimulus $S = (0,1,1)$ in the low (Figure 5G) and high (Figure 5I) concentration cases is the amplitudes of the transients and not which PNs are firing at a high (>0.5), moderate (~0.4) or low (<0.3) rate. For example, PNs firing at moderate rates are 2 and 3 when $S = (1,0,0)$ (Figure 5D), 1 and 2 when $S = (0,0,1)$ (Figure 5E), and 5 and 6 when $S = (1,1,1)$ (Figure 5F), while none of the PNs fire at moderate rates when $S = (0,1,1)$ (Figure 5G–I).

The temporal aspect of the coding is complicated by the fact that olfactory networks in real insect systems exhibit rhythmic oscillations of ~20–30 Hz (Wehr and Laurent, 1996). Thus, for example, the first one or two oscillations could be transients with the remaining oscillations representing a periodic equilibrium that remains in effect until the stimulus is removed or the ORNs become adapted to prolonged input. This idea can only be tested, however, if sufficient data are collected over long enough time intervals to distinguish initials transients from long-run cycles. Further, the meaning of transients can only be gauged if the state of the antennal lobes (or olfactory bulb in vertebrates) is known prior to each stimulation. Thus it is important to evaluate spike trains for sufficiently long periods of time before, during and after stimulation to evaluate initial, transient and final lobe states associated with particular stimuli. It is possible that the antennal lobe is reset to some initial condition by a regulating signal originating in another part of the brain (e.g. a memory center in the mushroom bodies), or that the lobe may revert to some kind of background noise state after stimulation and be in this state prior to receiving ORN input in response to the next stimulus. If one stimulus follows immediately after another, however, then the initial state for the second stimulus is the final state for the first, so the situation becomes quite complex unless initial transients are not part of the olfactory code.

Stopfer *et al.* (1997) recently demonstrated that odor discrimination in honey bees remains functional, but at a degraded level of resolution, when synchrony between antennal lobe and mushroom body oscillations is disrupted through the application of picrotoxin to the brains of individual workers. A reason for this loss of resolution might be that the mushroom body neuropil receiving PN input may depend on synchronized antennal lobe/mushroom body oscillations for timing the beginning of a transient input signal. If this were the case, then in the absence of the synchronizing oscillations the start of the transients would no longer be read correctly (i.e. from a mathematical perspective, no way exists to mark the initial state of the network and the appropriate initial condition is lost). Implicit in this hypothesis is the assumption that similar odors are more likely to have similar transients that would then be confused in the absence of a precise timing mechanism. On the other hand, very different odors would have dissimilar transients that would still be discriminable even if the timing mechanism were no longer precise, provided the stimuli were applied for a sufficiently long period of time. This idea is supported by the transients in Figure 5D–F that, for very different stimuli, are quite distinct even though the initial and final (equilibrium) PN values are the same for all stimuli.

The network constructed here does exhibit oscillations for some sets of parameters, and is more likely to oscillate as the delay parameters are increased in value. A thorough investigation of sets of parameters that produce oscillations of the type observed *in vivo* still needs to be undertaken, with attention being paid to the importance of inputs terms I_j and I_k in equations (4) (Appendix A), since these inputs would include feedback from other parts of the brain that may send entraining, cohering, reinforcing or timing signals. Further, it is clear from our analysis that we need empirical investigations on how the brain may reset the electrical activity of the antennal lobe prior to coding, because an internally consistent set of initial conditions is required for the production of a precise coding of odor quality.

Conclusion

In the introduction, we raised several questions associated with the olfactory processing problem in general, as well as insects in particular. The results we report here shed some light on the specific questions and give us pause for thought on the general questions. In terms of the network we use here to model olfactory processing in the insect antennal lobe, our results demonstrate that, comparably speaking, signal attenuation (decay) has a moderate effect, PN–IN feedback has a large effect and a strong nonlinearity in the activation function (i.e. a steep slope) has an overwhelming effect on the network's ability to produce discriminable, concentration invariant, odor codes. Thus, a consistent theme that emerges from our results is that the stronger the nonlinearities in the network the more distinct the code appears to be. These nonlinearities reduce the likelihood that neurons maintain intermediate response values and cause neurons to either be 'on' (close to 1) or 'off' (close to 0). Further, high PN–IN feedback synapse values help maintain the code after the stimulus has been removed. Note that it takes only 30 neurons confined to binary 'on–off' states to code the quality of over one billion (2^{30}) different odors. Finally, the network model presented here provides a unique tool for investigating the role of nonlinearities in the response of ORNs to mixtures versus pure odorants, although we have yet to conduct a systematic analysis of this question.

The process of running the model and trying to interpret the output raises a number of general issues that are critical for our understanding of olfactory coding in animals. The first issue relates to the initial state of the lobe or bulb (i.e. just prior to stimulation). The second issue is the amount of time it takes for the lobe or bulb to make the transition from the initial state to the particular state that represents the concentration-independent coding for the stimulus at hand. The third issue is the dynamic nature of the code itself (is the code an equilibrium state, a stable oscillation or a transitory pattern). The fourth issue is a function of the oscillations that occur in the lobe, their source and their relationship to the code itself.

In our simulations, in the absence of empirical information on the nature of the 'resting' states of the insect antennal lobe, the initial conditions we used were half way between no activity and maximum activity for each of the neurons in the network. Clearly more comprehensive empirical studies are needed on resting versus coding states of all the neurons involved. Such studies would also provide insights into the kind of time constants associated with the transitions from resting to coding states. Further, the relationship between these time constants and observed frequencies of oscillations should help clarify the role of the oscillations in coding itself and whether the combinatorial hypothesis of Laurent and colleagues is a viable paradigm for olfactory coding.

The similarities between odor processing in all animals imply that investigation of the insect olfactory coding problem provides insight into olfactory processing in all animals. This study represents a first attempt at investigating how effectively the basic architecture of the insect olfactory lobe is able to form a stable concentration-independent code that solves the olfactory coding problem in insects. The network we model performs exceptionally well for the small homogeneous stimulus space considered here. In future studies, we need to account for the dynamic properties of ORNs, as well as present more challenging situations in terms of the dimensionality and heterogeneity (spatial and temporal) of the stimulus space. Such studies will provide us with a better understanding of the limitations of the network employed here in solving more complex problems. They will also

provide insights into how the power of our network to form stable olfactory codes is affected by scaling (inclusion of more glomeruli, etc.). Finally, as is clear from the four issues discussed above, network models play a very useful role in identifying what aspects of the biology are most critical for obtaining a better understanding of olfactory processing in all animals.

Acknowledgements

We thank Bill Lemon for helpful discussions, Benjamin Mattei for technical comments, Jean-Pierre Rospar and anonymous reviewers for extensive comments and suggestions on how to improve our presentation, and Barry Ache for patiently but insistently ensuring that our paper is readable to biologists.

References

Ache, B.W. (1991) *Phylogeny of smell and taste*. In Getchell, T.V., Doty, R.L., Bartoshuk, L.M. and Snow, J.B. (eds), Smell and Taste in Health and Disease. Raven Press, New York , pp. 3–18.

Akers, R.P. and **Getz, W.M.** (1992) *A test of identified response classes among olfactory receptors in the honeybee worker*. Chem. Senses, 17, 191–209.

Akers, R.P. and **Getz, W.M.** (1993) *Response of olfactory sensory neurons in honey bees to odorants and their binary mixtures*. J. Comp. Physiol., 173, 169–185.

Aradi, I. and **Erdi, P.** (1996) *Multicompartmental Modeling of the Olfactory Bulb*. Cybernetics and Systems, 27, 605–615.

Arnold, G., Masson, C. and **Budharugsa, S.** (1985) *Comparative study of the antennal lobes and their afferent pathway in the worker bee and the drone* (Apis mellifera*)*. Cell Tissue Res., 242, 593–605.

Atema, J., Borroni, P., Johnson, B., Voigt, R. and **Handrich, L.** (1989) *Adaptation and mixture interaction in chemoreceptor cells: mechanisms for diversity and contrast enhancement*. In Laing, D.G. (ed.), Perception of Complex Smells and Tastes. Academic Press, Marrickville, pp. 83–100.

Av-Ron, E. and **Rospars, J.-P.** (1995) *Modeling insect olfactory neuron signaling by a network utilizing disinhibition*. Biosystems, 36, 101–108.

Av-Ron, E. and **Vibert, J.-F.** (1996) *A model for temporal and intensity coding in insect olfaction by a network of inhibitory neurons*. Bio-Systems, 39, 241–250.

Av-Ron, E., Parnas, H. and **Segel, L.A.** (1991) *A minimal biophysical model for an excitable and oscillatory neuron*. Biol. Cybernet., 45, 487–500.

Bäck T., Fogel, D.B. and **Michalewicz, Z. (eds)** (1997) Handbook of Evolutionary Computation. Oxford University Press, Oxford.

Baird, B. (1986) *Nonlinear dynamics of pattern formation and pattern recognition in the rabbit olfactory bulb*. Physica D, 22, 150–175.

Barnard, E. (1989) *Analysis of the Lynch–Granger model for olfactory cortex*. Biol. Cybernet., 62, 151–155.

Bhalla, U.S. and **Bower, J.M.** (1993) *Exploring parameter space in detailed single neuron models: simulations of the mitral and granule cells of the olfactory bulb*. J. Neurophysiol., 69, 1948–1965.

Boeckh, J. and **Ernst, K.D.** (1987) *Contribution of single unit analysis in insects to an understanding of olfactory function*. J. Comp. Physiol. A, 161, 549–565.

Boeckh, J., Distler, P., Ernst, K.D., Hösl, M. and **Malun, D.** (1990) *Olfactory bulb and antennal lobe*. In Schild, D. (ed.), Chemosensory Information Processing. Springer-Verlag, Berlin, pp. 201–227.

Bower, J.M. (1991) *Piriform cortex and olfactory object recognition*. In Davis, J.L. and Eichenbaum, H. (eds), Olfaction: A Model System for Computational Neuroscience. The MIT Press, Cambridge, MA, pp. 265–285.

Christensen, T.A. and **Hildebrand, J.G.** (1987) *Functions, organization, and physiology of the olfactory pathways in the lepidopteran brain*. In Gupta, A.P. (ed.), Arthropod Brain: Its Evolution, Development, Structure, and Functions. Wiley, New York, pp. 457–484.

Christensen, T.A., Waldrop, B.R., Harrow, I.D. and **Hildebrand, J.G.** (1993) *Local interneurons and information processing in the olfactory glomeruli of the moth* Maduca sexta. J. Comp. Physiol. A, 173, 385–399.

Davis, L. (ed.) (1990) Handbook of Genetic Algorithms. Van Nostrand Reinhold, New York.

Delaney, K.R., Gelperin, A., Fee, M.S., Flores, J.A., Gervais, R., Tank, D.W. and **Kleinfeld, D.** (1994) *Waves and stimulus-modulated dynamics in an oscillating olfactory network*. Proc. Natl Acad. Sci. USA, 91, 669–673.

Derby, C.D., Girardot, M., Daniel, P.C. and **Fine-Levy, J.B.** (1989) *Olfactory discrimination of mixtures: behavioral, electrophysiological and theoretical studies using the spiny lobster* Panulirus argus. In Laing, D.G., Cain, W.S., McBride, R.L. and Ache, B.W. (eds), Perception of Complex Smells and Taste. Academic Press, Orlando, FL, pp. 65–82.

Dittmer, K., Grasso, F. and **Atema, J.** (1995) *Effects of varying plume turbulence on temporal concentration signals available to orienting lobsters*. Biol. Bull., 189, 232–233.

Érdi, P., Aradi, I. and **Gröbler, T.** (1997) *Rhythmogenesis in single cells and population models: olfactory bulb and hippocampus*. BioSystems, 40, 45–53.

Fine-Levy, J.B. and **Derby, C.D.** (1992) *Behavioral discrimination of binary mixtures and their components: effects of mixture interactions on coding of stimulus intensity and quality*. Chem. Senses, 17, 307–323.

Flanagan, D. and **Mercer, A.R.** (1989a) *An atlas 3-d reconstruction of the antennal lobes in the worker honey bee,* Apis mellifera (*Hymenoptera: Apidea)*. Int. J. Insect Morphol. Embryol., 18, 145–159.

Flanagan, D. and **Mercer, A.R.** (1989b) *Morphology and response characterstics of neurones in the deutocerebrum of the brain in the honeybee* Apis mellifera. J. Comp. Physiol. A, 164, 483–494.

Fonta, C., Sun, X.-J. and **Masson, C.** (1991) *Cellular analysis of odour integration in the honey bee antennal lobe*. In Goodman, L.J. and Fisher, R.C. (eds), The Behaviour and Physiology of Bees. CAB International, Wallingford, pp. 227–241.

Fonta, C., Sun, X.-J. and **Masson, C.** (1993) *Morphology and spatial distribution of bee antennal lobe interneurones responsive to odours*. Chem. Senses, 18, 101–119.

Freeman, W.J. and **Skarda, C.A.** (1985) *Spatial EEG patterns, non-linear dynamics and perception: the neo-Sherringtonian view*. Brain Res. Rev., 10, 147–175.

Fujimura, K., Yokohari, F. and **Tateda, H.** (1991) *Classification of antennal olfactory receptors of the cockroach,* Periplaneta americana *L*. Zool. Sci., 8, 243–255.

Gascuel, J. and **Masson, C.** (1991) *A quantitative unltrastructural study of the honeybee antennal lobe*. Tissue Cell, 23, 341–355.

Getz, W.M. (1991) *A neural network for processing olfactory-like stimuli*. Bull. Math. Biol., 53, 805–823.

Getz, W.M. (1994) *Odor processing in the insect olfactory system*. In World

Congress on Neural Networks—San Diego. Lawrence Erlbaum Associates and INNS Press, Hillsdale, NJ, pp. 661–668.

Getz, W.M. and **Akers, R.P.** (1993) *Olfactory response characteristics and tuning structure of placodes in the honey bee* Apis mellifera. Apidologie, 24, 195–217.

Getz, W.M. and **Akers, R.P.** (1994) *Honey bee olfactory sensilla behave as integrated processing units*. Behav. Neural Biol., 61, 191–195.

Getz, W.M. and **Akers, R.P.** (1995) *Partitioning nonlinearities in the response of honey bee olfactory receptor neurons to binary odors*. BioSystems, 34, 27–40.

Getz, W.M. and **Akers, R.P.** (1997) *Response of American cockroach* (Periplaneta americana*) olfactory receptors to selected alcohol odorants and their binary combinations*. J. Comp. Physiol. A, 180, 701–709.

Getz, W.M. and **Chapman, R.F.** (1987) *An odor discrimination model with application to kin recognition in social insects*. Int. J. Neurosci., 32, 963–967.

Getz, W.M. and **Page, R.** (1991) *Chemosensory communication systems and kin recognition in honey bees*. Ethology, 87, 298–315.

Granger, R., Ambrose-Ingerson, J., Antón, P.S., Whitson, J. and **Lynch, G.** (1990) *Computational action and interaction of brain networks*. In Zornetzer, S.F., Davis, J.L. and Lau, C. (eds), An Introduction to Neural and Electronic Networks. Acadmic Press, San Diego, CA, pp. 25–41.

Hammer, M. and **Menzel, R.** (1995) *Learning and memory in honeybees*. J. Neurosci., 15, 1617–1630.

Hansson, B.S., Ljungberg, H., Hallberg, E. and **Löfstedt, C.** (1992) *Functional specialization of olfactory glomeruli in a moth*. Science, 256, 1313–1315.

Hansson, B.S., Anton, S. and **Christensen, T.A.** (1994) *Structure and function of antennal lobe neurons in the male turnip moth,* Agrotis segetum (*Lepidoptera: Notuidae)*. J. Comp. Physiol. A, 175, 547–562.

Haykin, S. (1994) Neural Networks: A Comprehensive Foundation. Macmillan College Publishing, New York.

Hendin, O., Horn, D. and **Hopfield, J.J.** (1994) *Decomposition of a mixture of signals in a model of the olfactory bulb*. Proc. Natl Acad. Sci. USA, 91, 5924–5946.

Hildebrand, J.G. and **Shepherd, G.M.** (1997) *Mechanisms of olfactory discrimination: converging evidence for common principles across phyla*. Annu. Rev. Neurosci., 20, 595–631.

Homberg, U., Christiansen, T.A. and **Hildebrand, J.G.** (1989) *Structure and function of the deutocerebrum in insects*. Annu. Rev. Entomol., 34, 477–501.

Hopfield, J.J. (1991) *Olfactory computation and object perception*. Proc. Natl Acad. Sci. USA, 88, 36462–36466.

Joerges, J., Küttner, A., Galizia, C.G. and **Menzel, R.** (1997) *Representations of odours and odour mixtures visualized in the honeybee brain*. Nature, 387, 285–288.

Kaissling, K.E. (1987) R.H. Wright Lectures on Insect Olfaction. Edited by Konrad Colbow, Simon Fraser University, Burnaby, British Columbia, Canada.

Kang, J. and **Caprio, J.** (1997) In vivo *responses of single olfactory receptor neurons of channel catfish to binary mixtures of amino acids*. J. Neurophysiol., 1, 1–8.

Kleinfeld, D., Delaney, K.R., Fee, M.S., Flores, J.A., Tank, D.W. and **Gelperin, A.** (1994) *Dynamics of propagating waves in the olfactory network of a terrestrial mollusk: an electrical and optical study*. J. Neurophysiol., 72, 1402–1429.

Koza, J.R. (1992) Genetic Programming. MIT Press, Cambridge, MA.

Laurent, G. (1996) *Dynamical representation of odors by oscillating and evolving neural assemblies*. Science, 274, 976–979.

Laurent, G. and **Davidowitz, H.** (1994) *Encoding of olfactory information with oscillating neural assemblies*. Science, 265, 1872–1875.

Laurent, G. and **Narghi, M.** (1994) *Odorant-induced oscillations in the mushroom bodies of the locust*. J. Neurosci., 14, 2993–3004.

Laurent, G., Wehr, M. and **Davidowitz, H.** (1996) *Temporal representations of odors in an olfactory network*. J. Neurosci., 16, 3837–3847.

Lemon, W.C. and **Getz, W.M.** (1997) *Temporal resolution of general odor pulses by olfactory sensory neurons in American cockroaches*. J. Exp. Biol., 200, 1809–1819.

Lemon, W.C and **Getz, W.M.** (1999) *Responses of cockroach antennal projection neurons to pulsatile olfactory stimuli*. Ann. N.Y. Acad. Sci., 855, 517–520.

Li, Z. (1990) *A model of olfactory adaptation and sensitivity enhancement in the olfactory bulb*. Biol. Cybernet., 62, 349–361.

Li, Z. and **Hopfield, J.J.** (1989) *Modeling the olfactory bulb and its neural oscillatory processings*. Biol. Cybern., 61, 379–392.

Linster, C. and **G. Dreyfus** (1996) *A model for pheromone discrimination in the insect antennal lobe: investigation of the role of neuronal response pattern complexity*. Chem. Senses, 21, 19–27.

Linster, C. and **Hasselmo, M.** (1997) *Modulation of inhibition in a model of olfactory bulb reduces overlap in the neural representation of olfactory stimuli*. Behav. Brain Res., 84, 117–127.

Linster, C. and **Masson, C.** (1996) *A neural model of olfactory sensory memory in the honeybee's antennal lobe*. Neural Computat., 8, 94–114.

Linster, C. and **Smith, B.H.** (1997) *A computational model of the response of honey bee antennal lobe circuitry to odor mixtures: overshadowing, blocking and unblocking can arise from lateral inhibition*. Behav. Brain Res., 87, 1–14.

Linster, C., Kerszberg, M. and **Masson, C.** (1994) *How neurons may compute: the case of insect sexual pheromone discrimination*. J. Computat. Neurosci., 1, 231–238.

Linster, C., Masson, C., Kerszberg, M., Personnaz, L. and **Dreyfus, G.** (1993) *Computational diversity in a formal model of the insect olfactory macroglomerulus*. Neural Computat., 5, 228–241.

MacLeod, K. and **Laurent, G.** (1996) *Distinct mechanisms for synchronization and temporal encoding patterning of odor-encoding assemblies*. Science, 274, 976–979.

Malaka, R., Ragg, T. and **Hammer, M.** (1995) *Kinetic models of odor transduction implemented as artificial neural networks—simulations of complex response properties of honeybee olfactory neurons*. Biol. Cybernet., 73, 195–207.

Malaka, R., Schmitz, S. and **Getz, W.M.** (1996) *A self-organizing model of the antennal lobes*. In Maes P., Mataric M.J., Meyer J.-A., Pollack J. and Wilson, S.W. (eds), From Animals to Animats 4: Proceedings of the Fourth International Conference on Simulation of Adaptive Behaviour. MIT Press, Cambridge, MA, pp. 45–54.

Malun, D. (1991a) *Synaptic relationships between GABA-immunoreactive neurons and an identified uniglomerular projection neuron in the antennal lobe of* Periplaneta americana*: a double-labeling electron microscope study*. Histochemistry, 96, 197–207.

Malun, D. (1991b) *Inventory and distribution of synapses of identified*

uniglomerular projection neurons in the antennal lobe of Periplaneta americana. J. Comp. Neurol., 305, 348–360.

Masson, C. and **Linster, C.** (1995) *Towards a cognitive understanding of odor discrimination: combining experimental and theoretical approaches*. Behav. Process., 35, 63–82.

Masson, C. and **Mustaparta, H.** (1990) *Chemical information processing in the olfactory system of insects*. Physiol. Rev., 70, 199–245.

Menzel, R., M.Hammer, G. Braun, J.Mauelshagen, M.Sugawa (1991) *Neurobiology of learning and memory in honeybees*. In Goodman, L.J. and Fisher, R.C. (eds), The Behaviour and Physiology of Bees. CAB International, Wallingford.

Meredith, M. (1992) *Neural circuit computation: complex patterns in the olfactory bulb*. Brain Rese. Bull., 29, 111–117.

Michelson, H.B. and **Wong, R.K.S.** (1991) *Excitatory synaptic response mediated by $GABA_A$ receptors in the hippocampus*. Science, 253, 1420–1423.

Moore, P.A. and **Atema, J.** (1988) *A model of a temporal filter in chemoreception to extract directional information from a turbulent odor plume*. Biol. Bull., 174, 355–363.

Moore, P.A. and **Atema, J.** (1991) *Spatial information in the three-dimensional fine structure of an aquatic odor plume*. Biol. Bull., 181, 408–418.

Murlis, J. (1986) *The structure of odor plumes*. In Payne, T.L., Birch, M.C. and Kennedy, C.E.J. (eds), Mechanisms in Insect Olfaction. Oxford University Press, Oxford, pp. 27–38.

Murlis, J., Elkington, J.S. and **Cardé, R.T.** (1992) *Odor plumes and how insects use them*. Annu. Rev. Entomol., 37, 505–532.

Osorio D., Getz, W.M. and **Rybak, J.** (1994) *Insect vision and olfaction: different neural architectures for different kinds of sensory signals?* In Cliff, D., Husbands, P., Meyer J.-A. andWilson, S.W. (eds), From Animals to Animats 4: Proceedings of the Fourth International Conference on Simulation of Adaptive Behaviour. MIT Press, Cambridge, MA, pp. 74–80.

Press, W.H., Flannery, B.P., Teukolsky, S.A. and **Vetterling, W.T.** (1986) Numerical Recipes: The Art of Scientific Computing. Cambridge University Press, Cambridge, p. 818.

Rospars, J.P. (1983) *Invariance and sex-specific variations of the glomerular organization in the antennal lobes of a month, mamestra brassicae, and a butterfly,* Pieris brassicae. J. Comp. Neurol., 220, 80–96.

Rospars, J.P. (1988) *Structure and development of the insect antennodeutocerebral system*. Int. J. Insect Morphol. Embryol., 17, 243–294.

Rospars, J.-P. and **Fort, J.-C.** (1994) *Coding of odour quality: roles of convergence and inhibition*. Computat. Neural Sys., 5, 121–145.

Rospars, J.P. and **Hildebrand, J.G.** (1992) *Anatomical identification of glomeruli in the antennal lobes of the male sphinx moth* Maduca sexta. Cell Tissue Res., 270, 205–227.

Sass, H. (1978) *Olfactory receptors on the antenna of* Periplaneta*: response constellations that encode food odors*. J. Comp Physiol., 128, 227–233.

Schild, D. and **Riedel, H.** (1992) *Significance of glomerular compartmentalization for olfactory coding*. Biophys. J., 61, 704–715.

Segev, I. (1992) *Single neurone models: oversimple, complex and reduced*. Trends Neurosci., 15, 414–415.

Selzer, R. (1984) *On the specificities of antennal olfactory receptor cells of* Periplaneta americana. Chemical Senses, 8, 375–395.

Shepherd, G. M. (1994) Neurobiology, 3rd edn. Oxford University Press, New York.

Skarda, C.A. and **Freeman, W.J.** (1987) *How brains make chaos in order to make sense of the world*. Behav. Brain Sci., 10, 161–195.

Smith, B.H. and **Getz, W.M.** (1994) *Non-pheromomal olfactory processing in insects*. Annu. Rev. Entomol., 39, 351–375.

Souček, B. (ed.) 1992) Dynamic, Genetic, and Chaotic Programming. John Wiley & Sons, New York.

Stopfer, M., Bhagavan, S., Smith, B.H. and **Laurent, G.** (1997) *Impaired odour discrimination on desynchronization of odour-encoding neural assemblies.* Nature, 390, 70–74.

Sun, X.-J., Fonta, C. and **Masson, C.** (1993) *Odour quality processing by bee antennal lobe neurons*. Chem. Senses, 18, 355–377.

Vareschi, E. (1971) *Duftunterscheidung bei der Honigbiene—Einzelzell-Ableitungen und Verhaltensreaktionen*. Z. Vergl. Physiol., 75, 143–173.

Wang, D., Buhmann, L. and **von der Malsburg, C.** (1991) *Pattern segmentation in associative memory*. In Davis, J.L. and Eichenbaum, H. (eds), Olfaction: A Model System for Computational Neuroscience. The MIT Press, Cambridge, MA, pp. 213–224.

Wang, X.J. and **Rinzel, J.** (1992) *Alternating and synchronous rhythms in reciprocally inhibited model neurons*. Neural Computat., 4, 84–97.

Wehr, M. and **Laurent, G.** (1996) *Odour encoding by temporal sequences of firing in oscillating neural assemblies*. Nature, 384, 162–166.

White, J., Hamilton, K.A., Neff, S.R. and **Kauer, J.S.** (1992) *Emergent properties of odor information coding in a representational model of the salamander olfactory bulb*. J. Neurosci., 12, 1772–1780.

Yokoi, M., Mori, K. and **Nakanishi, S.** (1995) *Refinement of odor molecule tuning by dendrodendritic synaptic inhibition in the olfactory bulb*. Proc. Natl Acad. Sci. USA, 92, 3371–3375.

Accepted February 9, 1999

Appendix

A. Underlying equations

The simplest way of characterizing the state of the jth neuron in a net of n neurons (i.e. $j = 1, \ldots, n$) is through the single variable v_j, which can be regarded as the voltage or activation potential that is simultaneously the same value at all points on the neuron. Thus, from a conductance point of view, the neuron has no spatial structure or extent. Obviously this is a gross simplification, with spatial structure playing a crucial role in integrating input from highly arborized dendrites. At the most basic level, however, finite propagation speeds of spikes, of currents or of changes in voltage along neurons have a spatial dimension that can be incorporated into the model through explicit time delays. Such time delays also capture some of the delay characteristics associated with the operation of chemical synapses between the neurons themselves.

Having defined an activation potential v_j, we assume that the output V_j of the jth neuron (interpreted as the spiking rate for spiking neurons) is related to the activation potential through a nonlinear activation function $\phi_h(v_j)$ of type h; that is,

$$V_j = \phi_h(v_j) \tag{1}$$

Note the subscript h allows for the fact that more than one type or class of activation functions may exist. For spiking neurons, we assume that V_j is scaled to take values on the interval [0,1], where 0 represents no activity and 1 the maximum firing rate. In this case ϕ_h is a monotonically increasing mapping of the real line $(-\infty,+\infty)$

onto the compact interval [0,1]. A commonly used activation function that has this property is the logistic equation

$$\phi(v_j) = \frac{1}{1 + e^{-\beta_h(v_j - \theta_h)}} \tag{2}$$

where $\beta_h > 0$ and θ_h are constants that respectively determine how closely ϕ_h approximates a step function (ϕ_h approaches a step function as $\beta_h \to \infty$) and where the step occurs (the step occurs around $v_j = \theta_h$).

If the jth neuron is efferent to m other neurons with spiking rates V_k, $k = 1, \ldots, m$, and is also activated by some other source I_j (this may also include a propensity to fire spontaneously, although in this context, I_j and the parameter θ_h in expression 2 are functionally interchangeable). then the standard electrical circuit equations, discretized with respect to time (setting and selecting the units of t so that the maximum firing rate in each time interval is 1—i.e. the unit of t is ~3–5 ms and will be regarded here as exactly 5 ms), are

$$v_j(t+1) = \mu_j v_j(t) + \sum_{k=1}^{m} w_{jk} V_k(t - \delta_{kj}) + I_j, \quad j = 1, \ldots, m \tag{3}$$

where w_{jk} represent the strengths of the synapses of the m neurons afferent to the neuron in question and δ_{kj} is a time delay associated with how long it takes to transmit information on the state of the kth neuron to the jth neuron (it is assumed to take on the value of 0 or integer values of time). Note that if the jth neuron has a capacitance C_j and resistance R_j, then, in terms of electrical circuit theory [e.g. discretize equation (14.14) in Haykin (1994)], the parameter μ_j in equation (3) is $\mu_j = 1 - 1/(C_j R_j)$. The sign of each determines whether the kth neuron inhibits or excites the jth neuron.

Equation (3) is generic and reflects no special architecture. It is easily specialized to account for the antennal lobe architecture depicted in Figure 1 and discussed in the text as follows. We use the symbols X_i, Y_j and Z_k to denote the spiking rates of the ORNs (receptor neurons), INs (intrinsic neurons) and PNs (projection neurons) respectively (Figure 1), and let x_i, y_j and z_k denote the corresponding activation potentials. As alluded to above, we do not include a dynamic model for generating the ORN action potentials x_i, but only model the dynamics of the IN and PN action potentials y_j and z_k respectively. We treat ORN spiking rates, X_i, directly as given constant inputs. This allows us to study the dynamic properties of the antennal lobe network without the confounding influence of dynamic ORN inputs. Once the computational properties of antennal lobe network are better understood, then the effects of more realistic ORN input can be studied using dynamics models of ORN responses (e.g. see Av-Ron and Rospars, 1995; Av-Ron and Vibert, 1996) to constant and temporally varying stimuli using available data (Lemon and Getz, 1997) as a basis for developing the ORN component of the model.

In the spirit of initially avoiding confounding complexities, we assume that all INs have the same activation function ϕ_1 (i.e. expression 2 with $h = 1$) and all PNs have the same activation function ϕ_2 (i.e. expression 2 with $h = 2$). Thus, equation (3) for our specific architecture reduces to the two sets of equations

$$y_j(t+1) = \mu_j y_j(t) + \sum_{l=1}^{n} w_{li} \phi_1\left(y_l(t - \delta_{lj})\right) + \sum_{i \in \text{Type}j} \tilde{w}_{ij} X_i(t) + \hat{w}_j \phi_2\left(z_j(t - \hat{\delta}_j)\right) + I_j, \quad j = 1, \ldots, m$$

$$z_k(t+1) = \bar{\mu}_k z_k(t) + \bar{w}_k \phi_1\left(y_k(t - \bar{\delta}_k)\right) + \bar{I}_k, \quad k = 1, \ldots, n \tag{4}$$

where the tildes, hats and bars are used to indicate the level at which the various synapse, decay and delay parameters apply (Figure 1). For example, $\tilde{w}_{ij} \geq 0$ are the excitatory synapse weights between the ORNs and INs, $w_{lj} \leq 0$ are the inhibitory synapse weights among the INs, $\hat{w}_{ij} \leq 0$ are the inhibitory synapses weights between the INs and their corresponding PNs, and $\bar{w}_{ij} \geq 0$ is the synapse weight for the excitatory feedback of the PNs onto their corresponding INs. The terms I_j and $\bar{I}_k$ are the background excitation of the INs and PNs respectively. These background levels could be due to self-excitation, unaccounted input from neurons or effects of placement parameters θ_h, $h = 1, 2$, in expression (2) (since we set $\theta_h = 0$ for all neurons, as mentioned earlier we can incorporate the effects of nonzero θ_h by adding the real value of θ_h to the corresponding excitation term—cf. equations 2 and 3).

B. Network output and performance measures

The output from the network is the responses of the PNs which will vary depending on the particular input stimulus, as well as the values of the network parameters. These latter values are the dimension n of the model itself, the activation (β_1, β_2, θ_1, θ_2), decay (μ_j, $\bar{\mu}_j$, j, $k = 1, \ldots, n$), delay (δ_{lj}, $\hat{\delta}_{ij}$, $\bar{\delta}_{ij}$, j, k, $l = 1, \ldots, n$), and weighting parameter (w_{lj}, $\tilde{w}_{ij}$,$\hat{w}_j$, w_j, where j in our case represents a sensory receptor of type j and j, k, $l = 1, \ldots, n$) parameters values, as well as on the values of the external/self-activating inputs (I_j, $\bar{I}_k$, j, $k = 1, \ldots, n$). As mentioned above, these inputs and and the activation threshold parameters θ_1 and θ_2 effectively enter the equations in the same way (i.e. the effects of changes in the value of the activation thresholds θ_1 and θ_2 can also be accomplished by making appropriate changes to the values of I_j and $\bar{I}_k$—cf. equations 2 and 3). Thus, in our model, we set θ_1 and θ_2 to zero and manipulate only the values of the inputs and to obtain a network 'background' state that facilitates coding, as described in more detail below. In reality, however, we should not expect the activation position parameters θ_1 and θ_2 to be zero and need to take this into account when trying to obtain empirical measurements of the external/self-activating inputs I_j and $\bar{I}_k$. The total set of parameters can be written as

$$P = \{\beta, \theta, \mu, \bar{\mu}, \Delta, \hat{\delta}, \bar{\delta}, \mathbf{W}, \tilde{\mathbf{W}}, \hat{\mathbf{w}}, \bar{\mathbf{w}}, \mathbf{I}, \bar{\mathbf{I}}\}$$

where the symbols are matrices (uppercase W) and vectors of the corresponding subscripted italicized symbols introduced above.

To permit the temporal structure in the response of the PNs to be taken into account over the 400 ms response interval motivated in the main text, we divide this response into eight 50 ms bins (Figure 2). Thus, if our iteration unit of time is 5 ms and the output from the jth PN in response to a 100 ms input stimulus S_q is given by (cf. equation 2)

$$Z_j(t) = \varphi_2(z_j(t)), \text{ for } t = 1, \ldots, 8 \tag{5}$$

(i.e. $t \in [0,400$ ms], where $z_j(t)$ is the solution to equation 4), then this output can be aggregated into the eight-dimensional vector (Figure 2)

$$\mathbf{p}_{jq} = \left(p_{1jq}, p_{2jq}, \ldots, p_{8jq}\right) \text{ where } p_{ijk} = \sum_{t=10(i-1)+1}^{10i} Z_j(t) \text{ for } i = 1,\ldots,8 \quad (6)$$

(Note, for notational simplicity, we have not indexed the fact that the network output variables z_j and Z_j also depend on stimulus S_q.) If we then concatenate the output across all n PNs (Figure 2), we have the input/output relationship that each stimulus, S_q, produces as an N-dimensional vector $\mathbf{P}_q = (\mathbf{p}_{1q}, \ldots, \mathbf{p}_{nq})$, where, in this case, $N = i \times n = 48$ ($i = 8$, $n = 6$).

Simple ways to compare two output vectors $\mathbf{P}_1$ and $\mathbf{P}_2$ is to take a vector norm (city block, square root of sum of squares, or maximum element, etc.) of the difference between these two vectors (Figure 2). Alternatively, we can interpret the directions of the vectors as coding odor quality and the magnitudes as coding for concentration and then train the network to optimize its performance in classifying input stimuli of the same quality as the same or discriminating between different odors irrespective of concentration.

The most appropriate way to measure the performance of a network, such as the one represented by equations (1–3), is to evaluate how well the network is able to code for quality independent of concentration and to discriminate among odors of different quality. In many situations the measure of interest is the proportion of errors that are made in misclassifying the quality of an odor or not discriminating between different odors (Getz and Page, 1991). These measures, however, require that *a priori* we specify a threshold (or equivalently a level of tolerance for variations in odors of the 'same' quality which is also a level of resolution for discriminating among odors of 'different' quality) (e.g. see Getz and Akers, 1997). Because plotting the performance of the system in terms of this threshold variable greatly increases that computational work, as well as the graphical complexity of the results, we will only present the results here in terms of average measures of verity of quality and resolution of discrimination. This simplification in no way affects our ability to address the issues at hand.

Suppose we idealize an environment to contain M odors O_q, $q = 1, \ldots, M$, each of which occurs at one of three concentrations C_1, C_2 and C_3, where the first is relatively low, the second is medium and the third is relatively high. Note that these odors may have different component odorants, or may have the same components occurring in different concentrations (i.e. the ratio of concentrations of components differs from one odorant to the next). Let S_q^i represent the 100 ms stimulus comprising odor q at, say, three concentrations $i = 1, 2, 3$ (in ascending strengths: low, medium, high), and let $\mathbf{P}_q^i$ represent the corresponding 400 ms output from the network. Then, to ensure that the output is as invariant as possible with respect to concentration, we are interested in minimizing the differences in the directions of these two vectors (e.g. in minimizing differences between $\mathbf{P}_q^1$ and $\mathbf{P}_q^3$, assuming $\mathbf{P}_q^2$ falls somewhere between $\mathbf{P}_q^1$ and $\mathbf{P}_q^2$ when concentration 2 is intermediate between concentrations 1 and 3—see Figure 2 and cf. Getz and Chapman (1987). Thus the problem of selecting a set of network parameters P that maintains a sense of quality can be expressed as [any norm can be used, e.g. Euclidean (see Figure 2), but the actual norm we used in our calculations was the absolute value]:

$$\min_P \left\{ Q = \frac{1}{NM} \sum_{q=1}^{M} \left\| \frac{\mathbf{P}_q^1}{\left\|\mathbf{P}_q^1\right\|} - \frac{\mathbf{P}_q^3}{\left\|\mathbf{P}_q^3\right\|} \right\| \right\} \quad (7)$$

Note that the measure is scaled by the number of comparisons M, as well as the length N of the output vectors (recall $N = 48$, being six concatenated vectors each having eight time bins of spiking rates averaged over 50 ms intervals). By contrast, if we want to focus on maximizing the ability of the network to discriminate between pairs of odors all at, say, the medium concentration (i.e. concentration 2), then we can select the parameters that solve the following maximization problem:

$$\max_P \left\{ D = \frac{2}{NM(M-1)} \sum_{q_1=1}^{M} \sum_{q_2=q_1+1}^{M} \left\| \frac{\mathbf{P}_{q1}^2}{\left\|\mathbf{P}_{q1}^2\right\|} - \frac{\mathbf{P}_{q2}^2}{\left\|\mathbf{P}_{q2}^2\right\|} \right\| \right\} \quad (8)$$

Finally, if we want to consider a criterion that simultaneously accounts for verity of quality across different concentrations of the same odor as well as discriminability among odors of different quality, we can select the parameters to solve the problem:

$$\max_P \left\{ R = \frac{D}{Q} \right\} \quad (9)$$

Considering that Q is a measure of the average distance between stimuli of the same odor quality and D is the average distance between stimuli of different odor qualities, the network could not begin to distinguish between odors of the different qualities at the same concentration or odors of the same quality at different concentrations unless $R > 1$, and could not perform very well unless $R > 1$.

C. Three odorant simulations

The following equations characterize the response of six classes of sensory neurons, three linear specialist and three linear differencers, to the three odorant stimulus $S = (C_1, C_2, C_3)$:

$$X_1 = C_1, \quad X_2 = C_2, \quad X_3 = C_3, \quad X_4 = |C_1 - C_2|, \quad X_5 = |C_1 - C_3|, \quad X_6 = |C_2 - C_3| \quad (10)$$

Thus, in response to a 100 ms input stimulus of the second odorant at concentration C, the three input variables X_i, $i = 1$, 3 and 5, are zero over the whole 400 ms computational interval, while the three input variables X_i, $i = 2$, 4 and 6, are equal to C for $0 \le t \le 100$ ms and 0 for the remaining 300 ms interval. In response to a 0.5:0.5 mixture of the first and third odorants at total concentration C, however, inputs X_i, $i = 2$ and 5, are zero over the whole computational interval, while X_i, $i = 1$, 3, 4 and 6 are equal to C/2 for $0 \le t \le 100$ ms and 0 for the remaining 300 ms interval.

The analyses involved training the network to the following predefined set of stimuli, characterized in terms of two response rate parameters C^0 and ΔC. The stimuli were chosen to span a given range of concentrations in a way that would allow us to control for the effect of concentration in a rigorous manner. They were also chosen to span a range of odor qualities that included

pure odorants, equicomponent binary mixtures and an equicomponent blend of all three odorants. More particularly, we defined $C^- = C^0 - \Delta C$ and $C^+ = C^0 + \Delta C$, and defined the following 13 stimuli using a more informative superscript notation than that used in equations (7) and (8) [the correspondence between the two notations is relatively clear: superscripts 1, 2 and 3 in performance measures (7) and (8) are replaced by superscripts –, 0 and +, and the number of stimuli used to generate performance measure (7) is $M = 3$ and performance measure (8) is $M = 7$]:

$$S_1{}^i = (C^i,0,0), \quad S_2{}^i = (0,C^i,0), \quad S_3{}^i = (0,0,C^i) \quad \text{for } i = -, 0, + \tag{11a}$$

$$S_4{}^0 = (C^0/2,C^0/2,0), \quad S_5{}^0 = (C^0/2,0,C^0/2), \quad S_6{}^0 = (0,C^0/2,C^0/2) \tag{11b}$$

and

$$S_7{}^0 = (C^0/3,C^0/3,C^0/3) \tag{11c}$$

As discussed in the section above, each of these 13 stimuli that we used as input to equations (4) produced the corresponding output vectors $\mathbf{P}_q{}^i$, $i = -, 0, +$, $q = 1, 2, 3$ and $\mathbf{P}_q{}^0$, $q = 4, \ldots, 7$. We used the output pairs $(\mathbf{P}_q{}^-, \mathbf{P}_q{}^+)$, $q = 1, 2, 3$, to generate the quality measure Q defined in equation (7) and the outputs $\mathbf{P}_q{}^0$, $q = 1, \ldots, 7$, (21 pairs) to generate the discrimination measure D defined in equation (8).

The challenging problem remained to solve for sets of parameters P_Q, P_D and P_R that respectively optimize the performance measures Q, D and R, as defined in expressions (7–9), subject to appropriate constraints (e.g. the parameters must be non-negative). Once this was done, we could then compare these measures to see how well the system is able to produce a stable quality code, discriminate among different odors and simultaneously perform the two, somewhat conflicting, tasks. Since we anticipated that the network's ability to maintain quality would be eroded as the ratio $\Delta C/C$ increases from 0 to 1, we were motivated to compare the performance of the network for different values of C and ΔC.

D. Six odorant simulations

For this set of simulations the dimension of the odor space was increased from three to six, with stimuli now of the form $S = (C_1,C_2,C_3,C_4,C_5,C_6)$. As in the three-odorant case, we defined pure odorant stimuli at three different concentrations in terms of response rate parameters C^0 and ΔC. Specifically, we defined the 18 multiconcentration pure odorant stimuli (cf. equation 11a) as

$$S_1{}^i = (C^i,0,0,0,0,0), \ldots, S_6{}^i = (0,0,0,0,0,C^i), \quad \text{for } i = -, 0, + \tag{12a}$$

the fifteen single concentration equicomponent binary stimuli (cf. equation 11b) as

$$S_7{}^0 = (C^0/2,C^0/2,0,0,0,0), \ldots, S_{21}{}^0 = (0,0,0,0,C^0/2,C^0/2) \tag{12b}$$

and the single equicomponent full blend (cf. equation 11c) as

$$S_{22}{}^0 = (C^0/6,C^0/6,C^0/6,C^0/6,C^0/6,C^0/6) \tag{12c}$$

As in the three-odorant case, we used the corresponding output pairs $(\mathbf{P}_q{}^-,\mathbf{P}_q{}^+)$ $q = 1, 2, \ldots, 7$, to generate the quality measure Q defined in equation (7) and the outputs $\mathbf{P}_q{}^0$, $q = 1, \ldots, 22$ (231 pairs), to generate the discrimination measure D defined in equation (8). With six odorants, rather than the previous three, we needed to redefined the types of ORNs used to transduce chemical stimuli into electrical input (cf. equation 10).

The six classes of receptor neurons that we now used to produce the input into the network in terms of their response to the logarithmic concentrations C_i, $i = 1, \ldots, 6$, of the six odorants in question were (cf. equations 10):

$$X_1 = C_1 + C_2, \quad X_2 = C_3 + C_4, \quad X_3 = C_5 + C_6,$$
$$X_4 = |C_1 + C_3 - C_2 - C_4|$$
$$X_5 = |C_1 + C_5 - C_2 - C_6| \quad X_6 = |C_3 + C_5 - C_4 - C_6| \tag{13}$$

Note that, unlike the three-odorant case, we no longer have receptor neurons that specialize on any one single odorant. Thus this six-odorant case is a step up in complexity in addressing the problem of how well our relatively simple neural network is able to code the stimuli defined by expressions (12a–c).

E. Fixed and optimized parameter values

A number of different numerical routines exist for solving optimization problems (7–9) (Press *et al.*, 1986). Here we use a genetic algorithm (Davis, 1990; Koza, 1992; Souček, 1992; Bäck *et al.*, 1997) to solve these problems, since we are not only interested in the solutions P_Q, P_D and P_R that solve the three optimization problems (7–9) respectively, but how optimal solutions are approached through time. [The algorithm we used was written by W.M. Spear. We obtained the code in early August 1997 as freeware from the website http://www.aic.nrl.navy.mil/~spears/freeware.html. Spear describes the code as a standard genetic algorithm, similar to Grefenstette's work, employing Baker's SUS selection algorithm, with n-point cross-over maintained at 60%, a very low mutation rate, and selection based on proportional fitness.] This latter information may provide us with some insights into how the antennal lobes might learn to perform well in terms of whether quality identification or discrimination initially dominates. Further, we did not optimize over all parameters simultaneously, but we fixed some of the parameters in P and optimized over the rest. Through this approach, we hope to learn how different components of the network contribute to solving the olfactory processing problem in insects.

In the simulations discussed below, only the IN feedback parameters, w_{ij}, were free to mutate in the genetic algorithm. All the other network parameters were fixed and have the values list in Table 1. The initial conditions we used for the simulations were $y_j(0) = z_k(0) = 0.5$, $j, k = 1, \ldots, 6$. We did not use the relaxed (stable equilibrium) state as our initial condition because this state changes as the system evolves, and for some sets of parameters several relaxed states exist. If the system has only one relaxed state, we should expect the system to be in that state prior to stimulation. In reality, if the system has several relaxed states, then either its state prior to stimulation will be a function of its history or some mechanism may exist for setting the network to a particular initial state after each stimulation. The latter mechanism would be required if the coding was dependent not only on the stimulus involved but also on the initial state of the network.